

A Scaling Analysis of Frequency Dependent Energy Partition for Local and Regional Phases from Explosions

**John Murphy
Brian Barker
Jamil Sultanov**

**Science Applications International Corporation
10260 Campus Point Drive
San Diego, CA 92121**

Final Report

31 August 2007

APPROVED FOR PUBLIC RELEASE; DISTRIBUTION UNLIMITED.



**AIR FORCE RESEARCH LABORATORY
Space Vehicles Directorate
29 Randolph Road
AIR FORCE MATERIEL COMMAND
Hanscom AFB, MA 01731-3010**

NOTICE AND SIGNATURE PAGE

Using Government drawings, specifications, or other data included in this document for any purpose other than Government procurement does not in any way obligate the U.S. Government. The fact that the Government formulated or supplied the drawings, specifications, or other data does not license the holder or any other person or corporation; or convey any rights or permission to manufacture, use, or sell any patented invention that may relate to them.

This report was cleared for public release and is available to the general public, including foreign nationals. Qualified requestors may obtain additional copies from the Defense Technical Information Center (DTIC) (<http://www.dtic.mil>). All others should apply to the National Technical Information Service.

AFRL-VS-HA-TR-2007-1139 HAS BEEN REVIEWED AND IS APPROVED FOR
PUBLICATION IN ACCORDANCE WITH ASSIGNED DISTRIBUTION STATEMENT.

//Signature//

ROBERT J. RAISTRICK
Contract Manager

//Signature//

PAUL TRACY, Acting Chief
Battlespace Surveillance Innovation Center

This report is published in the interest of scientific and technical information exchange, and its publication does not constitute the Government's approval or disapproval of its ideas or findings.

REPORT DOCUMENTATION PAGE				Form Approved OMB No. 0704-0188	
Public reporting burden for this collection of information is estimated to average 1 hour per response, including the time for reviewing instructions, searching existing data sources, gathering and maintaining the data needed, and completing and reviewing this collection of information. Send comments regarding this burden estimate or any other aspect of this collection of information, including suggestions for reducing this burden to Department of Defense, Washington Headquarters Services, Directorate for Information Operations and Reports (0704-0188), 1215 Jefferson Davis Highway, Suite 1204, Arlington, VA 22202-4302. Respondents should be aware that notwithstanding any other provision of law, no person shall be subject to any penalty for failing to comply with a collection of information if it does not display a currently valid OMB control number. PLEASE DO NOT RETURN YOUR FORM TO THE ABOVE ADDRESS.					
1. REPORT DATE (DD-MM-YYYY) 31-08-2007		2. REPORT TYPE Final Report		3. DATES COVERED (From - To) 24-08-2004 to 23-08-2007	
4. TITLE AND SUBTITLE A Scaling Analysis of Frequency Dependent Energy Partition for Local and Regional Seismic Phases From Explosions		5a. CONTRACT NUMBER FA8718-04-C-0030			
		5b. GRANT NUMBER N/A			
		5c. PROGRAM ELEMENT NUMBER 62601F			
6. AUTHOR(S) J. R. Murphy, B. W. Barker and J. D. Sultanov*		5d. PROJECT NUMBER 1010			
		5e. TASK NUMBER SM			
		5f. WORK UNIT NUMBER A1			
7. PERFORMING ORGANIZATION NAME(S) AND ADDRESS(ES) Science Applications International Corporation 10260 Campus Point Drive San Diego, CA, 92121		8. PERFORMING ORGANIZATION REPORT NUMBER			
9. SPONSORING / MONITORING AGENCY NAME(S) AND ADDRESS(ES) Air Force Research Laboratory 29 Randolph Road Hanscom AFB, MA 01731-3010		10. SPONSOR/MONITOR'S ACRONYM(S) AFRL/RVBYE			
		11. SPONSOR/MONITOR'S REPORT NUMBER(S) AFRL-RV-HA-TR-2007-1111			
12. DISTRIBUTION / AVAILABILITY STATEMENT Approved for Public Release; Distribution Unlimited.					
13. SUPPLEMENTARY NOTES *Institute for Dynamics of the Geospheres, Russian Academy of Sciences					
14. ABSTRACT Seismic identification of small explosions relies on the application of discriminants that are effective in the regional distance range. The most reliable regional discriminants identified to date are those based on high frequency spectral ratios of the amplitudes of the regional shear phases Sn and Lg to those of the corresponding direct P phases Pn and Pg. However, the universal applicability of such discriminants remains in question because there is currently no physical model of S wave generation by explosions that has been shown to be quantitatively consistent with the range of available observations. The objectives of the research program summarized in this report have been to determine frequency dependent source scaling relations for observed regional P and S phases through statistical analyses of data recorded from underground nuclear explosions conducted at a variety of different test sites, and to apply these derived scaling relations to a quantitative evaluation of the credibility of various proposed source mechanisms for generation of the regional shear phases Sn and Lg observed from underground explosion sources. The source scaling results obtained have been found to be remarkably consistent, indicating that the observed Sn and Lg spectra scale with yield in a manner which is very comparable to that of the corresponding direct Pn spectra, generally differing significantly only over narrow frequency bands defined by differences in the P and S wave corner frequencies. These results provide strong constraints which must be satisfied by any plausible proposed physical mechanism of explosion S wave generation.					
15. SUBJECT TERMS Nuclear Explosions, S Waves, Source Scaling, Semipalatinsk, Lop Nor, Novaya Zemlya, NTS, Mueller/Murphy					
16. SECURITY CLASSIFICATION OF:			17. LIMITATION OF ABSTRACT	18. NUMBER OF PAGES	19a. NAME OF RESPONSIBLE PERSON
a. REPORT UNCLASSIFIED	b. ABSTRACT UNCLASSIFIED	c. THIS PAGE UNCLASSIFIED			Robert Raistrick
			SAR	50	19b. TELEPHONE NUMBER (include area code) 781-377-3726

Table of Contents

1. Introduction	1
2. Background	2
3. Technical Approach	8
3.1 Signal Processing and Statistical Analysis Procedures	8
3.2 Description of a Mueller/Murphy Based Model For Scaling of Explosion S/P Spectral Ratios	10
4. Results and Discussion	11
4.1 Semipalatinsk	12
4.2 Lop Nor	23
4.3 Novaya Zemlya	26
4.4 NTS	31
5. Conclusions	38
References	41

Figures

1. Comparison of the predicted decrease in Rg excitation as a function of explosion source depth (left) with the corresponding depth dependence of direct P predicted by the Mueller/Murphy explosion source model (right) for a nominal 5 kt explosion.

4
2. Comparison of broadband and bandpass filtered (0.5 – 1.5 Hz, 4.0 – 8.0 Hz) recordings of the Balapan test site explosions of 6/14/88 ($m_b = 4.8$, right) and 5/04/88 ($m_b = 6.1$, left) from station WMQ at a distance of about 8.5° . It can be seen that, although the broadband Lg/P ratios appear to be quite different for these two explosions, they are in fact quite similar when viewed through common narrow frequency bands.

5
3. Map locations of selected Soviet PNE tests which were recorded at the Borovoye station in Kazakhstan ($\Delta < 20^\circ$).

6
4. Comparison of the frequency-dependent yield (n) and depth (m) scaling exponents for Pn derived from the covariance analysis of Borovoye data recorded from the PNE events with the corresponding values predicted by the Mueller/Murphy explosion source model (Murphy et al, 2001).

7
5. Comparison of yield (top) and depth (bottom) frequency-dependent scaling exponents determined for the different regional phases recorded at Borovoye from the selected PNE events.

8
6. Mueller/Murphy based model for S/P spectral ratios where $S(f) \sim P(kf)$ and k represents the ratio of the P to S wave velocities of the source medium. The left panel shows the resulting P and S wave source functions for a nominal 20 kt explosion at normal containment depth in granite, while the right panel shows the corresponding predicted S/P spectral ratios.

10
7. Distribution of seismic stations used in the analysis of seismic source scaling from the various regional phases observed from underground nuclear explosions at the former Soviet Semipalatinsk test site (STS). Labeled stations are those for which high resolution digital data are available.

12
8. Vertical component digital data recorded at the Borovoye station (BRV, $\Delta \approx 650$ km) from a sample of Degelen Mountain nuclear explosions of known yield and depth of burial. The data are plotted as a function of apparent group velocity and in order of increasing yield between 1.1 and 78 kt.

13

9. Vertical component digital data recorded at the Borovoye station (BRV, $\Delta \approx 650$ km) from a selected sample of Balapan explosions encompassing a range of m_b extending from 4.8 to 6.2. The data are plotted as a function of apparent group velocity.	14
10. Example of a Borovoye explosion recording exhibiting numerous data spikes (top) and the same trace after processing it with a despiking routine (bottom).	15
11. Bandpass filter processing results for the Borovoye recording of the $m_b = 5.29$ Balapan nuclear explosion of 2/01/79, where the selected time windows for the Pn, Sn and Lg regional phases are indicated.	16
12. Comparison of observed Sn/Pn spectral ratios at station BRV for large and small Balapan explosions. These observed ratios are essentially identical, consistent with a frequency dependent magnitude scaling for Sn which must be very similar to that for Pn over this range of magnitude.	17
13. Comparison of observed Degelen Mountain Sn/Pn spectral ratios at station BRV as a function of source depth (left) and scaled depth (right).	17
14. Estimated yield scaling exponents (n) as a function of frequency for the Sn/Pn (left) and Lg/Pn (right) regional phase spectral ratios at station BRV for Degelen Mountain explosions. It can be seen that these inferred yield scaling exponents are quite small, differing from zero at the 95% confidence level only in a narrow frequency range from about 1 to 3 Hz.	18
15. Comparison of vertical component seismic recordings (left) and associated average S/P spectral ratios (right) for selected Degelen Mountain explosions with yields ranging from 1.5 to 90 kt recorded at the near-regional ($\Delta \approx 175$ km) station SEM.	19
16. Average observed Degelen Mountain explosion Sn/Pn (left) and Lg/Pn (right) peak amplitude ratios as a function of source to station azimuth for Soviet permanent network stations.	20
17. Comparison of frequency dependent yield scaling exponents (n) for the Degelen Sn/Pn Borovoye spectral ratios estimated from regressions with respect to yield (dashed) and m_b (solid).	21
18. Comparison of observed Degelen and Balapan frequency dependent yield scaling exponents for Sn/Pn (left) and Lg/Pn (right) with the theoretical exponents predicted by a simple source model based on Mueller/Murphy, with $Sn(f) = Pn(kf)$, where k represents the ratio of the P to S wave velocities of the source medium.	21

19. Comparison of observed Sn/Pn spectral ratios for two Balapan explosions of comparable yield, but significantly different long-period tectonic release characteristics (i.e. F factors). It can be seen that these observed spectral ratios show no statistically significant dependence on F in the 0.5 to 10 Hz frequency band.	23
20. Distribution of digital seismic stations used in the analysis of seismic source scaling of regional phases from Lop Nor explosions.	24
21. Bandpass filter processing results for the station AAK ($\Delta=10^\circ$) recording of the Lop Nor explosion of 29 July 1996.	24
22. Comparison of observed Lg/Pn spectral ratios at station MAK ($\Delta=7^\circ$) for Lop Nor explosions encompassing a wide range of source size.	25
23. Comparison of Lop Nor Lg/Pn spectral ratios as a function of m_b at 1.5 Hz. The left panel shows the measured phase spectral ratio values from the various stations while the right panel shows the corresponding station-corrected phase spectral ratio values obtained from the covariance analysis.	27
24. Comparison of observed Lop Nor and Balapan frequency dependent yield scaling exponents for Lg/Pn.	27
25. Comparison of observed Lop Nor frequency dependent yield scaling exponents for Lg/Pn with the theoretical exponents predicted by a simple source model based on Mueller/Murphy, with $S(f) = P(kf)$ where k represents the ratio of the P to S wave velocities of the source medium.	28
26. Near-regional Russian seismic stations for which high resolution digital data are available for selected Novaya Zemlya explosions.	29
27. Comparison of vertical component recordings of the Southern Novaya Zemlya explosions of 9/27/73 ($m_b = 5.9$, top) and 10/27/73 ($m_b = 7.0$, bottom) at near-regional station Amderma ($\Delta \approx 320$ km).	30
28. Comparison of Sn/Pn spectral ratios for Southern Novaya Zemlya explosions of 9/27/73 ($m_b = 5.9$) and 10/27/73 ($m_b = 7.0$) at stations Amderma (left) and Nar-yan-Mar (right).	30
29. Map showing the locations of the LLNL near-regional stations ELK, MNV, LAC and KNB, as well as the Yucca Flat testing area of NTS considered in the present study.	31

30. Vertical component digital data recorded at the Mina, Nevada LLNL network station (MNV, $\Delta \approx 240\text{km}$) from a selected sample of explosions detonated below the water table at Yucca Flat which encompass a range of m_b extending from 4.1 to 5.9.	32
31. Bandpass filter processing of the LLNL station MNV recording of the NTS explosion Techado ($m_b = 4.1$). It can be seen that the S wave spectral amplitude levels are above the P coda levels out to 10 Hz.	32
32. Comparison of LLNL network average S/P spectral ratios for selected explosions conducted below the water table at Yucca Flat. Solid lines denote the ratios corresponding to the smallest explosions (Techado, Borrego) while dashed lines denote the ratios corresponding to the larger explosions (Baseball, Scantling, Sandreef, Caprock, Dalhart).	33
33. Comparison of S/P spectral ratios estimated from LLNL station LAC recordings of small (Aleman) and large (Caprock) Yucca Flat explosions.	34
34. Comparison of theoretical S/P source spectral ratios predicted by the Mueller/Murphy based model for an overburied explosion in saturated tuff with a yield of 1 kt and a depth of burial of 550m and an explosion with a yield of 150 kt and a depth of burial of 650m.	35
35. Comparison of the ratio of the observed Aleman S/P ratio to the average S/P ratio for five larger Yucca Flat explosions having a mean m_b value of about 5.7 with the corresponding theoretical ratio predicted by the Mueller/Murphy based model.	36
36. Comparison of the ratio of the average observed S/P spectral ratio for the three smallest Yucca Flat explosions to the average observed S/P spectral ratio for five Yucca Flat explosions having a mean m_b value of about 5.7 with the corresponding theoretical ratio predicted by the Mueller/Murphy based model.	36
37. Ratios of station MNV S/P spectral ratios to corresponding network-averaged S/P spectral ratios for selected Yucca Flat explosions.	37
38. Average ratios of single station S/P spectral ratios to corresponding network-averaged S/P spectral ratios for LLNL stations ELK, KNB, LAC and MNV.	38

1. INTRODUCTION

It has long been recognized that teleseismic data alone are generally adequate for differentiating between underground nuclear explosions and earthquakes for seismic events down to about $m_b = 4.0$, which corresponds to what would be expected for a well-coupled 1 kt underground nuclear test conducted in a regional tectonic environment comparable to that of the Western U.S. (OTA, 1988). However, since it has been experimentally demonstrated that it is possible to reduce the amplitudes of the radiated seismic signals produced by low yield nuclear explosions by at least a factor of 70 by employing the cavity decoupling evasion scenario, it follows that comprehensive monitoring of underground nuclear tests in the 1 to 10 kt range will necessarily involve consideration of small seismic events having equivalent seismic magnitudes in the range $2.0 < m_b < 3.5$. Since such small events are generally not well-recorded teleseismically, event identification research in recent years has focused on the development of discriminants that are effective in the regional distance range. As a result of this research it has been found that the most reliable regional discriminants are those based on ratios of the amplitudes of the regional seismic shear phases Sn and Lg to those of the corresponding direct P phases Pn and Pg. More specifically, it has been demonstrated (Bennett and Murphy, 1986; Taylor et al, 1988; Fisk et al, 2002) that the high frequency (6-8 Hz) spectral ratio of P (Pn or Pg) to S (Sn or Lg) provides the most robust separation of underground explosions and earthquakes for small seismic events recorded at regional distances. While the experimental evidence for the power of this discriminant that has now been accumulated is compelling, a problem remains in that there is currently no physical model of S wave generation by explosions that has been shown to be quantitatively consistent with the wide range of observations from explosion sources (Stevens et al, 2003). Consequently, extrapolation of existing regional P/S discrimination criteria to previously untested locations and source conditions is still subject to significant uncertainty.

One factor that has contributed to the confusion regarding the applicability of various proposed models of S wave generation by explosions has been the lack of a uniform set of strong constraints that must be satisfied by any plausible physical mechanism. Consequently, the technical objectives of the research program summarized in this report have been to determine frequency dependent source scaling relations for observed regional P and S phases through statistical analyses of data recorded from underground nuclear explosions conducted at a variety of different test sites, and to apply these derived scaling relations to a quantitative evaluation of various proposed physical source mechanisms for generation of the regional shear phases Sn and Lg observed from underground explosion sources. The ultimate objective of the study is to attempt to improve U.S. operational nuclear monitoring capability by providing a quantitative framework which can be used to confidently evaluate expected regional event

discrimination performance as a function of the ranges of explosion size and emplacement conditions which must be considered in global nuclear monitoring.

This report provides a summary of investigations that have been conducted under this contract in order to derive improved quantitative constraints on proposed physical mechanisms for S wave generation by explosions. A brief review of previous work on this topic is presented in Section 2 where the characteristics of frequency dependent explosion source scaling are discussed and illustrated. This is followed in Section 3 by a discussion of the general technical approach to deriving frequency dependent source scaling relations using regional phase data observed from underground nuclear explosions. In Section 4, this technical approach is applied to regional phase data recorded from underground nuclear explosions conducted at the former Soviet Semipalatinsk and Novaya Zemlya test sites, the Chinese Lop Nor test site and the U.S. Nevada test site (NTS), and the derived scaling results are compared with the corresponding predictions of a simple phenomenological S/P source ratio model based on the Mueller/Murphy (1971) P wave explosion source model. The report concludes with Section 5, which contains a short summary and statement of conclusions regarding S wave generation by underground explosion sources.

2. BACKGROUND

A number of focused research studies have been conducted over the past several decades in attempts to better define the source of the S waves observed from underground nuclear explosions, particularly as they relate to the generation of the regional Lg phase which has come to play a central role in the identification and yield estimation of small explosions. In early studies of the seismic waves generated by underground nuclear explosions it was generally assumed that the observed S waves were produced by linear conversion of the primary explosion P waves by the layered geology in the source region and along the propagation path between the source and the receiver. However, it was soon recognized that relatively strong S arrivals were also observed on the transverse components of motion at regional distances and this necessitated the addition of a nonisotropic scattering mechanism to the simple linear conversion model. Subsequent deterministic simulations of the Lg phases produced by point source explosions in planar multilayered approximations of the crustal waveguide raised further questions regarding the plausibility of the linear P to S conversion mechanism in that isotropic explosions in high velocity source media such as granite were predicted to generate very little Lg energy (e.g. Jih and McLaughlin, 1988).

These inconsistencies prompted intensive searches for alternate sources of Lg which generally focused on either scattering of the Rg phase induced by the isotropic explosion into Lg (e.g. Gupta et al, 1991, 1997), or on direct generation of S and Rg waves by the non-isotropic components of the explosion source associated with spall and other nonlinear interactions of the primary explosion source with the overlying geology and free surface (e.g. Stevens et al, 1991, 2003). Although significant theoretical and observational evidence has been marshalled to support the plausibility of both of these hypothetical sources of Lg, problems remain in that neither seems completely consistent

with the wide range of Lg observational data which is currently available (Stevens et al, 2003). For example, it has been observed that Lg amplitude level correlates remarkably well with the known yields of underground explosions over broad source regions, and this fact seems difficult to reconcile with the Rg scattering hypothesis. Moreover, both of these proposed sources would predict a pronounced dependence of Lg excitation on source depth, and this seems inconsistent with the results of Nuttli (1986) and others who have obtained reliable Lg-based yield estimates for very deep explosions, including the U.S. Peaceful Nuclear Explosion (PNE) RULISON which was detonated at a scaled depth more than six times larger than the nominal Nevada Test Site (NTS) containment depth. It follows that additional research is needed to identify potential sources of explosion S and Lg phases which satisfy all available constraints.

One potentially powerful constraint on the source of S waves from explosions is provided by their frequency dependent scaling as a function of explosion yield, depth of burial and source medium, relative to the well-documented scaling of the associated direct P wave phases. That is, since it is well established that the scaling of the direct P waves observed from explosions can be explained to first order by a simple isotropic source model (Mueller and Murphy, 1971), the degree to which the scaling of secondary regional phases such as Sn and Lg is similar to that of the corresponding Pn phases provides direct evidence of any significant departures from the isotropic source model. For example, consider the hypothesis that Lg is generated by simple near-source scattering of the direct, explosion-induced Rg phase. Now for the relatively high frequencies of interest with respect to the Lg/P discriminant, the dependence of the explosion-induced Rg phase excitation on source depth can be approximated with good accuracy by considering the Rayleigh wave excitation in a homogeneous halfspace. For this case, it can be shown that the dependence of the Rayleigh wave displacement spectrum on explosion source depth, h , is given by (Bycroft, 1966; Murphy, 1973)

$$G(h) = e^{-\frac{\omega h}{\theta \gamma \alpha} \sqrt{1 - \gamma^2 \theta^2}} \quad (1)$$

where ω is the circular frequency, $\gamma = \beta/\alpha$ with β , α the compressional and shear wave velocities, respectively, and θ is the root of the characteristic equation corresponding to the velocity of Rayleigh wave propagation. Thus, at a fixed high frequency, Rg excitation is expected to decrease exponentially with increasing explosion source depth, with the rate of decrease increasing with frequency. This dependence is graphically illustrated in Figure 1 (left) which shows the predicted decrease in Rg excitation as a function of explosion source depth between 200 and 800m (normalized to a depth of 200m), for a frequency band extending from 1 to 10 Hz. Also shown on this figure (right) is the corresponding depth dependence for direct P predicted for the same range by the Mueller/Murphy explosion source model for a nominal 5kt explosion. It can be seen that these predicted dependencies on source depth are dramatically different for these two phases. It follows that a comparison of frequency dependent depth scaling exponents estimated from observed Pn and Lg phase data recorded from explosions at fixed test sites should provide very robust evidence regarding the plausibility of the proposed direct Rg scattering mechanism as the source of the Lg energy observed from explosion

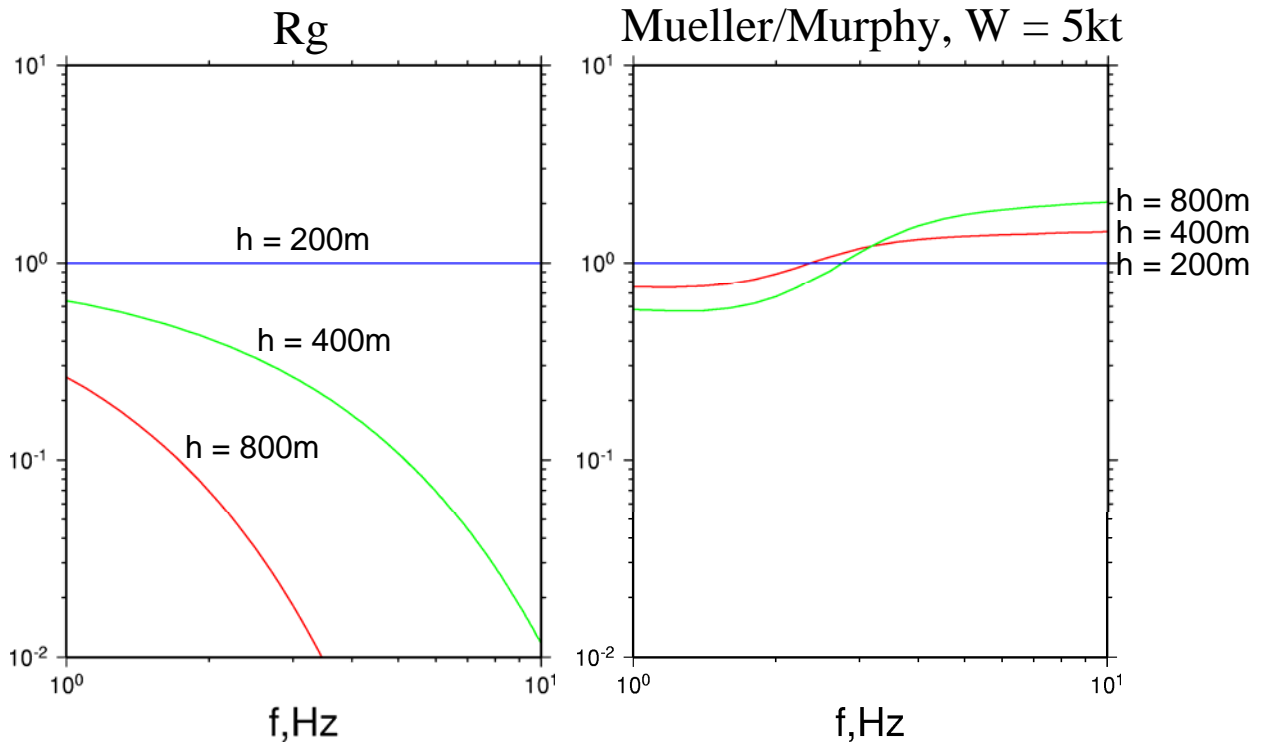


Figure 1. Comparison of the predicted decrease in Rg excitation as a function of explosion source depth (left) with the corresponding depth dependence of direct P predicted by the Mueller/Murphy explosion source model (right) for a nominal 5 kt

sources. Of course, more complex models of Rg scattering which consider the Rg induced by spall in addition to the direct explosion-induced Rg component might be expected to show a more complex dependence on source depth, but it too would have a characteristic dependence on explosion yield and depth which is likely to differ from that of direct P, and this simple example illustrates the potential resolving power provided by carefully defined scaling relations.

Similar comments apply to the hypothesis that the source of the explosion-induced Lg signal is related to the S waves generated by the non-isotropic components of the source associated with spall and other nonlinear interactions of the primary explosion source with the overlying near surface geology and free surface. In this case, the complexity of these nonlinear interactions makes it difficult to formulate even approximate yield and depth scaling rules such as those described above for Rg. However, it is known that the induced spall source does decrease with increasing scaled depth and, eventually, vanishes when the explosion is deep enough that no nonlinear interaction with the free surface occurs. Consequently, this component of the Lg source would be expected to decrease with increasing depth and to vanish at some large scaled depth which observationally appears to be in the range $500\text{-}700\text{m/kt}^{1/3}$, at which the U.S. PNE tests SALMON and RULISON were conducted. Once again, this expected depth dependence is quite different from that for direct P and, consequently, comparison of

derived P and Lg source scaling relations should provide a good test of the applicability of such proposed physical mechanisms for S wave generation by explosions.

Initial examination of broadband recordings from large and small explosions would seem to suggest that Lg does in fact scale differently with yield than Pn. This effect is illustrated in Figure 2 where it can be seen that the broadband Lg/Pn peak amplitude ratio at regional station WMQ for a Semipalatinsk explosion with $m_b = 6.1$ is much larger than the corresponding ratio observed at that same station for a smaller Semipalatinsk explosion with $m_b = 4.8$. However, this apparent difference in scaling is simply a result of the fact that the dominant frequency of Lg is lower than that of P, and that the low frequency amplitude levels decrease more rapidly with decreasing yield than those of the higher frequency components, in accord with the predictions of explosion source scaling models such as Mueller/Murphy. In fact, as is illustrated in this figure, when viewed in common narrow frequency bands, the Lg/P amplitude ratio appears to be approximately independent of yield.

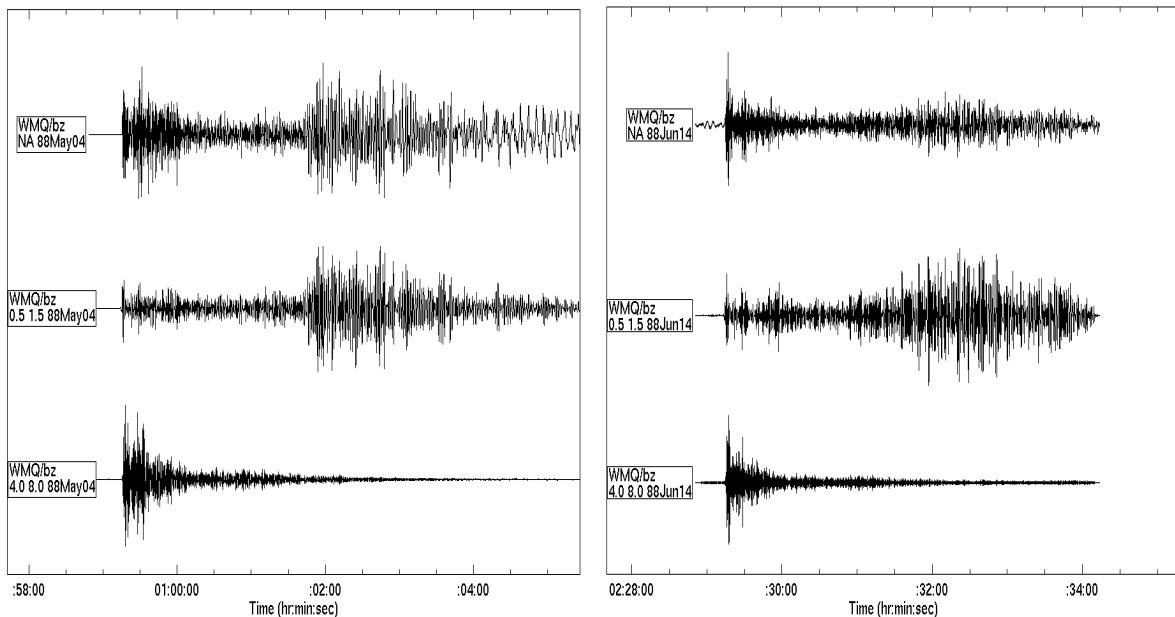


Figure 2. Comparison of broadband (top) and bandpass filtered (0.5 – 1.5 Hz center, 4.0 – 8.0 Hz bottom) recordings of the Balapan test site explosions of 6/14/88 ($m_b = 4.8$, right) and 5/04/88 ($m_b = 6.1$, left) from station WMQ at a distance of about 8.5° . It can be seen that, although the broadband Lg/P ratios appear to be quite different for these two explosions, they are in fact quite similar when viewed through common narrow frequency bands.

The selected examples of seismic source scaling presented above provide some qualitative insight into expected variations with explosion yield and depth of burial. However, in order to really constrain the source of the secondary shear arrivals it is necessary to analyze the frequency dependent scaling on a phase by phase basis using regional data recorded from explosions conducted under a wide variety of source conditions. One previous example of this approach was a study documented by Murphy

et al (2001), in which they analyzed the source scaling characteristics of regional phase data recorded at the Borovoye Geophysical Observatory in North Kazakhstan from a sample of 21 Soviet Peaceful Nuclear Explosions (PNE) of known yield and depth of burial. The map locations of these 21 explosions that are within 20° distance of the Borovoye station are shown in Figure 3, where it can be seen that they are widely distributed throughout the territories of the former Soviet Union. On the basis of prior experience (e.g. Mueller and Murphy, 1971) it was assumed in that analysis that the scaling of the explosion seismic source, $S(\omega)$, could be approximated using a functional relation of the form

$$S(\omega) \sim W^{n(\omega)} h^{m(\omega)} \quad (2)$$

where W and h are the explosion yield and depth of burial, respectively, and $n(\omega)$, $m(\omega)$ are the associated frequency dependent scaling exponents. The source scaling exponents estimated for the direct Pn phase from a covariance statistical analysis of the observed Borovoye PNE regional phase spectral amplitude data are displayed as a function of frequency in Figure 4 where they are compared over the frequency band from 0.5 to 5.0 Hz with the corresponding frequency dependent values predicted by the Mueller/Murphy model. It can be seen from this figure that these predicted yield and depth scaling exponents as a function of frequency are completely consistent with the experimentally determined values, at least within the rather large statistical uncertainty in these mean values. That is, as was noted previously for the corresponding teleseismic P wave data recorded from these same explosions, the observed frequency dependent scaling of the Pn spectral amplitude data with explosion yield and depth of burial are generally quite consistent with the predictions of the Mueller/Murphy explosion source scaling model.

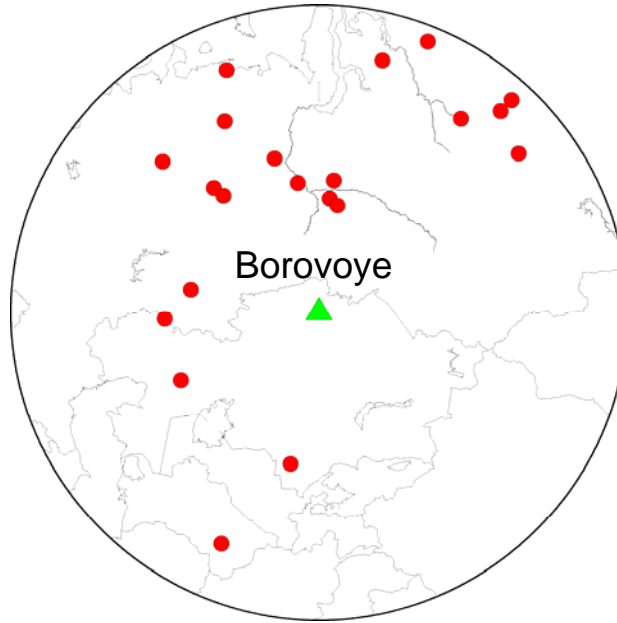


Figure 3. Map locations of selected Soviet PNE tests which were recorded at the Borovoye station in Kazakhstan ($\Delta < 20^\circ$).

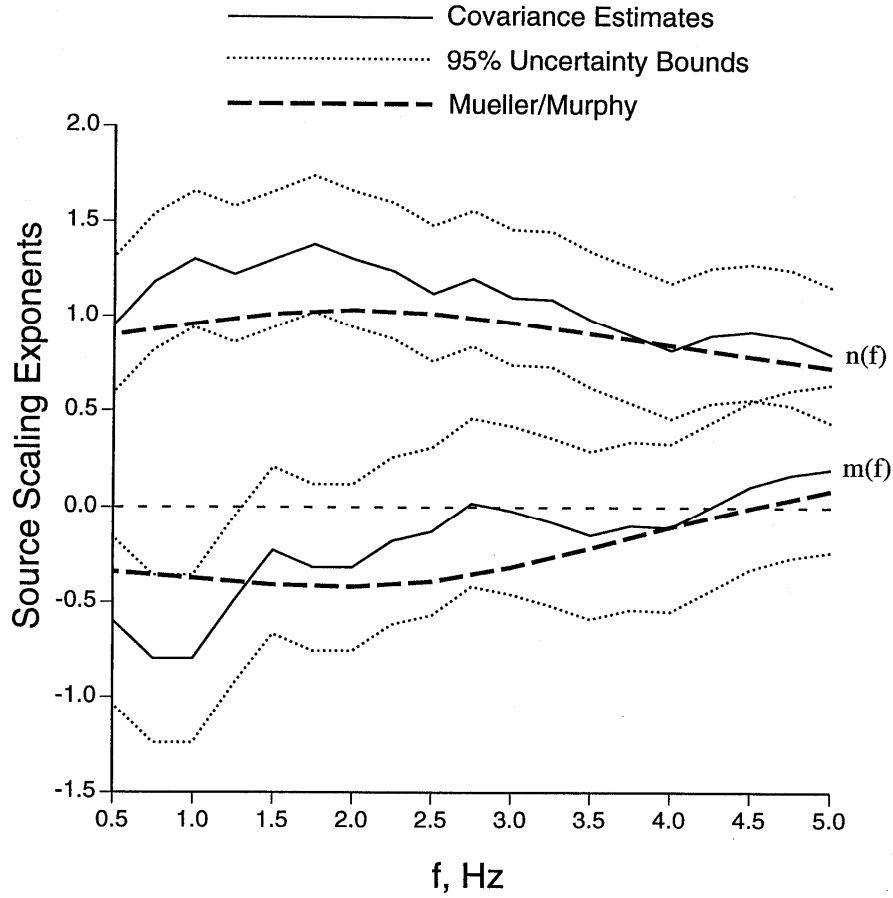


Figure 4. Comparison of the frequency-dependent yield (n) and depth (m) scaling exponents for Pn derived from the covariance analysis of Borovoye data recorded from the PNE events with the corresponding values predicted by the Mueller/Murphy explosion source model (Murphy et al, 2001).

The frequency dependent source scaling exponents derived for the four different secondary regional phases (i.e. Pcoda, Pg, Sn, Lg) are shown in Figure 5 where they are compared with those estimated for the direct Pn phase for both the yield (left) and depth (right) variables. It can be seen that the source scaling for all these regional phases are fairly similar over the frequency band extending from 0.5 to 5.0 Hz, particularly for the yield scaling exponents. The depth scaling exponents do however show some consistent differences between phases (e.g. Lg versus Pn) over the significant portions of this frequency range which could be indicative of differences in source mechanism. Unfortunately, Murphy et al (2001) concluded that the formal statistical uncertainty in these derived scaling exponents is too large to be able to conclude with high confidence that they are significantly different for the different regional phases. This lack of resolving power is at least partially due to the fact that these PNE events are widely distributed throughout the territories of the former Soviet Union (cf. Figure 3) and, consequently, propagation path variability makes it difficult to recover the source scaling

exponents with high accuracy. In the present program we minimize such propagation path variability by analyzing data recorded at specific stations from multiple explosions at fixed nuclear weapons test sites. This allows us to more precisely define any consistent differences in the source scaling of the various regional phases, which, in turn, provides much improved quantitative constraints on proposed source mechanisms for the secondary regional shear phases S_n and L_g .

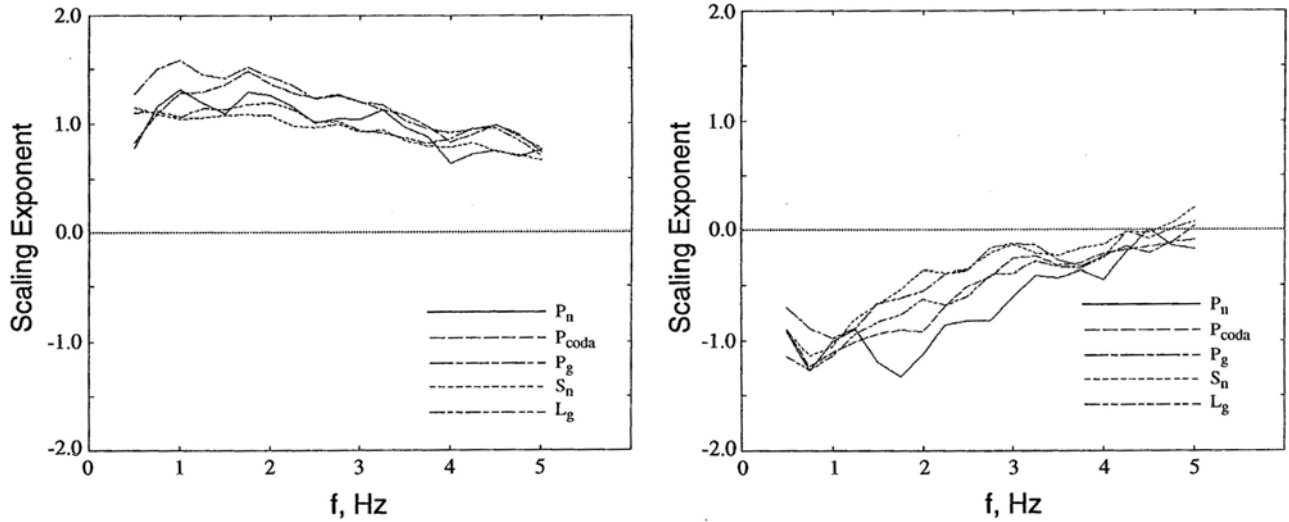


Figure 5. Comparison of yield (left) and depth (right) frequency-dependent scaling exponents determined for the different regional phases recorded at Borovoye from the selected PNE events.

3. TECHNICAL APPROACH

3.1 Signal Processing and Statistical Analysis Procedures

Following the precedent of Murphy et al (2001) and a number of other previous investigators, the regional phase spectral amplitudes used in this study were estimated using narrowband filter processing. In this approach, the recorded seismic data for each explosion are bandpass filtered using a Gaussian comb of filters spaced at intervals of 0.25 Hz between 0.5 and 10 Hz, where each filter is characterized by a Q value of $6f_c$, with f_c the filter center frequency. Filters of this type have been applied in a variety of previous explosion source scaling analyses (Murphy et al, 1989; Murphy et al, 2001; Murphy and Barker, 2001) and have been found to provide spectral estimates that are useful for purposes of seismic analyses. The spectral amplitude levels at each filter center frequency used in the source scaling studies have been determined by computing RMS values from the instrument-corrected filter outputs in each of the designated regional phase time windows.

Unlike the Soviet PNE explosions analyzed by Murphy et al (2001) that sampled a range of scaled depth (i.e. $h/W^{1/3}$) extending from about 200 to over 2000 $m/kt^{1/3}$, the

explosions at the nuclear weapons test sites considered in this study were generally conducted in a narrow range of scaled depths between about 100 and 130 m/kt^{1/3}. That is, the explosion source depth, h , is generally proportional to $W^{1/3}$ and, consequently, the depth dependence can be absorbed into a single frequency dependent yield scaling exponent. Therefore, for the purposes of the present analysis, equation (2) has been simplified to express the regional phase spectral ratios at a fixed station for explosions at a specific test site in the form

$$\frac{S_i(\omega)}{P_i(\omega)} = K(\omega)W_i^{n'(\omega)} \quad (3)$$

where here S corresponds to S_n or L_g and P to P_n or P_g , and $n'(\omega)$ denotes the difference in the frequency dependent yield scaling exponents, $n_s(\omega) - n_p(\omega)$, between the S and P phases. It follows that if the S wave source scales with yield in the same manner as the P wave source, the estimated $n'(\omega)$ values are expected to be close to zero. Any differences in depth dependence between the different regional phases can then be assessed in terms of observed departures from the average ratios predicted by equation (3).

Taking the logarithms of both sides of equation (3) leads to the linear relation

$$\log \left[\frac{S(\omega)}{P(\omega)} \right]_i = \tilde{K}(\omega) + n'(\omega) \log W_i \quad (4)$$

that can be solved for $n'(\omega)$ and $\tilde{K}(\omega)$ using linear least squares, given a set of regional phase spectral ratio observations from explosions of known yield. Equation (4) is directly applicable to testing areas like Degelen and NTS where yields of individual explosions encompassing a wide yield range are known. However, for testing areas such as Balapan, Lop Nor and Novaya Zemlya where individual yields are generally not known, teleseismic body wave magnitudes are used as surrogates for yield, assuming that the slope, b , of the average test site m_b /yield relation

$$m_b = C + b \log W \quad (5)$$

is known. That is, the dependence of the observed regional phase spectral amplitude ratios on m_b is estimated statistically to obtain $n'(\omega)/b$, and then the corresponding frequency dependent yield scaling exponents, $n'(\omega)$, are approximated using the known value of b . It will be demonstrated in the next section that these two procedures give very comparable results when applied to a common set of Degelen explosions for which both yields and m_b values are known.

3.2 Description of a Mueller/Murphy Based Model For Scaling of Explosion S/P Spectral Ratios

It will be shown in the following section that the source scaling effects on the observed S/P spectral ratios for all of the nuclear test sites considered in this study are remarkably consistent with a simple phenomenological model first proposed by Fisk et al (2005) in which the seismic source for S is defined to be directly proportional to the corresponding Mueller/Murphy P wave source, with a corner frequency reduced by the S/P velocity ratio of the source medium. This model is graphically illustrated in the left panel of Figure 6, which shows the Mueller/Murphy P wave source, $P(f)$, for a nominal 20 kt explosion at normal containment depth in granite, together with an S wave source given by $S(f) \sim P(kf)$ where $k = \alpha/\beta$, with α, β the compressional and shear wave velocities of the source medium. In this example, the constant of proportionality has been set to two for display purposes. The right hand panel of Figure 6 shows the corresponding theoretical S/P spectral ratio, which is constant at low frequency, and then decreases with increasing frequency between the S and P wave corner frequencies to a constant lower value above the P wave corner frequency. Because Mueller/Murphy is an ω^2 model, the difference between the low and high frequency asymptotic levels is given by $(\alpha/\beta)^2$, or approximately a factor of 3 for typical hardrock media.

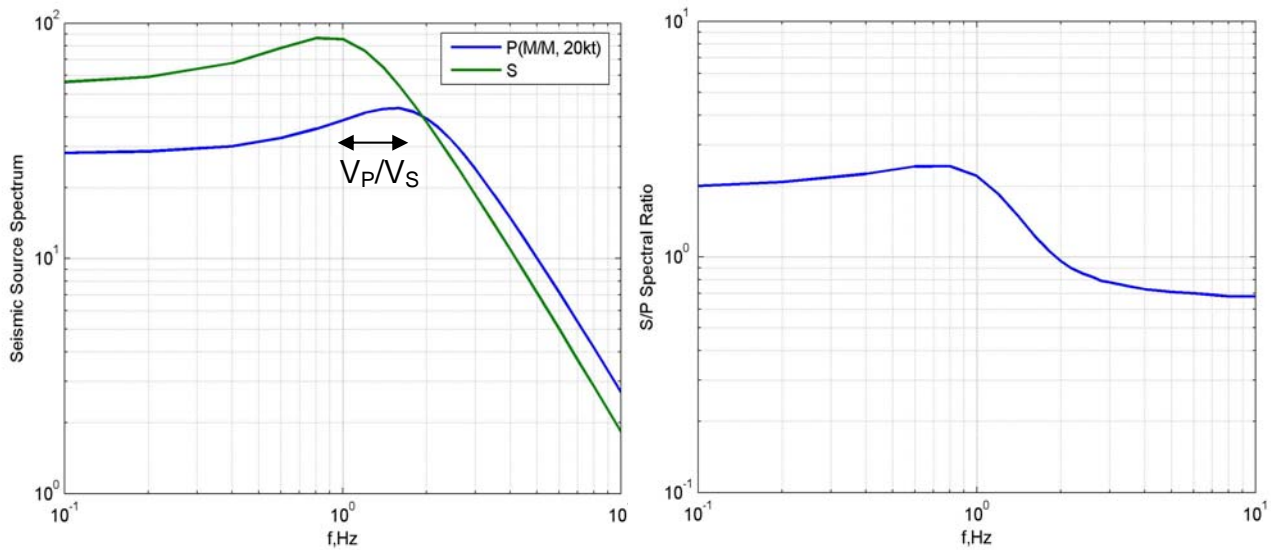


Figure 6. Mueller/Murphy based model for S/P spectral ratios where $S(f) \sim P(kf)$ and k represents the ratio of the P to S wave velocities of the source medium. The left panel shows the resulting P and S wave source functions for a nominal 20 kt explosion at normal containment depth in granite, while the right panel shows the corresponding predicted S/P spectral ratios.

The implications of this model with respect to explosion source scaling of the S/P spectral ratios can be quantified using the following simple formulation. At any fixed regional station, the observed P and S wave displacements, $Z_p(\omega)$ and $Z_s(\omega)$, from explosions at a particular testing area can be represented schematically in the form

$$Z_p(\omega) = S_p(\omega, W, h) \cdot T_p(\omega) \quad Z_s(\omega) = S_s(\omega, W, h) \cdot T_s(\omega) \quad (6)$$

where T_p , T_s denote the frequency dependent propagation path effects and S_p , S_s the explosion source functions for P and S, respectively. It follows that the S/P spectral ratio is given by

$$\frac{S(\omega)}{P(\omega)} = \frac{Z_s(\omega)}{Z_p(\omega)} = \frac{S_s(\omega, W, h)}{S_p(\omega, W, h)} \cdot \frac{T_s(\omega)}{T_p(\omega)} \quad (7)$$

For our approximate scaling model

$$\begin{aligned} S_p(\omega, W, h) &= \text{Mueller/Murphy P Source} \\ S_s(\omega, W, h) &= E_s(\omega, W, h) \cdot S_p(k\omega, W, h) \end{aligned} \quad (8)$$

where $k = \alpha/\beta$ for the source medium and it is assumed that the frequency dependent S/P source excitation ratio, $E_s(\omega, W, h)$ is independent of W, h at a fixed test site (i.e)

$$E_s(\omega, W, h) = E_s(\omega) \quad (9)$$

It follows that for a fixed station and test site, the S/P ratio for a particular explosion having yield W and depth of burial h can be expressed as

$$\left. \frac{S(\omega)}{P(\omega)} \right|_{W, h} = E_s(\omega) \cdot \frac{S_p(k\omega, W, h)}{S_p(\omega, W, h)} \cdot \frac{T_s(\omega)}{T_p(\omega)} \quad (10)$$

and, consequently, the source scaling of the S/P spectral ratio between two explosions with different yields and depths of burial can be written as

$$\frac{S/P(\omega, W_2, h_2)}{S/P(\omega, W_1, h_1)} = \frac{S_p(k\omega, W_2, h_2)/S_p(\omega, W_2, h_2)}{S_p(k\omega, W_1, h_1)/S_p(\omega, W_1, h_1)} \quad (11)$$

That is, this phenomenological model predicts that the scaling of the observed S/P spectral ratios with W, h at a given station for explosions at a fixed test site depends only on the Mueller/Murphy P wave source scaling model and the P to S velocity ratio of the source medium. In the following section this simple model will be applied to theoretical simulations of the observed source scaling of S/P spectral ratios at the various test sites considered in this study.

4. RESULTS AND DISCUSSION

In this section, the technical approach described in Section 3 above is applied to analyses of the source scaling characteristics of regional phase observations from underground nuclear explosions at the former Soviet Semipalatinsk and Novaya Zemlya test sites, the Chinese Lop Nor test site and the U.S. NTS test site.

4.1 Semipalatinsk

The analysis of source scaling of regional phase spectral ratios for underground nuclear explosions at the Semipalatinsk test site has focused on data recorded at the stations shown on the map of Figure 7 from explosions at the Degelen Mountain and Balapan testing areas of that test site. On this map the labeled stations denote those for which high resolution digital data are available, while the unlabeled stations are Soviet permanent network stations for which parametric peak amplitude phase ratio data have been compiled. The most important of these stations is the Borovoye Geophysical Observatory (BRV), which is one of the oldest digitally recording seismic stations in the world, having initiated digital recording in 1966 (Adushkin and An, 1990). Vertical component data recorded at station BRV at a distance of about 650 km from selected explosions at the Degelen Mountain and Balapan testing areas are shown in order of increasing source size in Figures 8 and 9, respectively. As was noted previously, individual yields and depths of burial have been announced for a significant number of Degelen explosions, while generally only seismic measures of source size (i.e. m_b) are

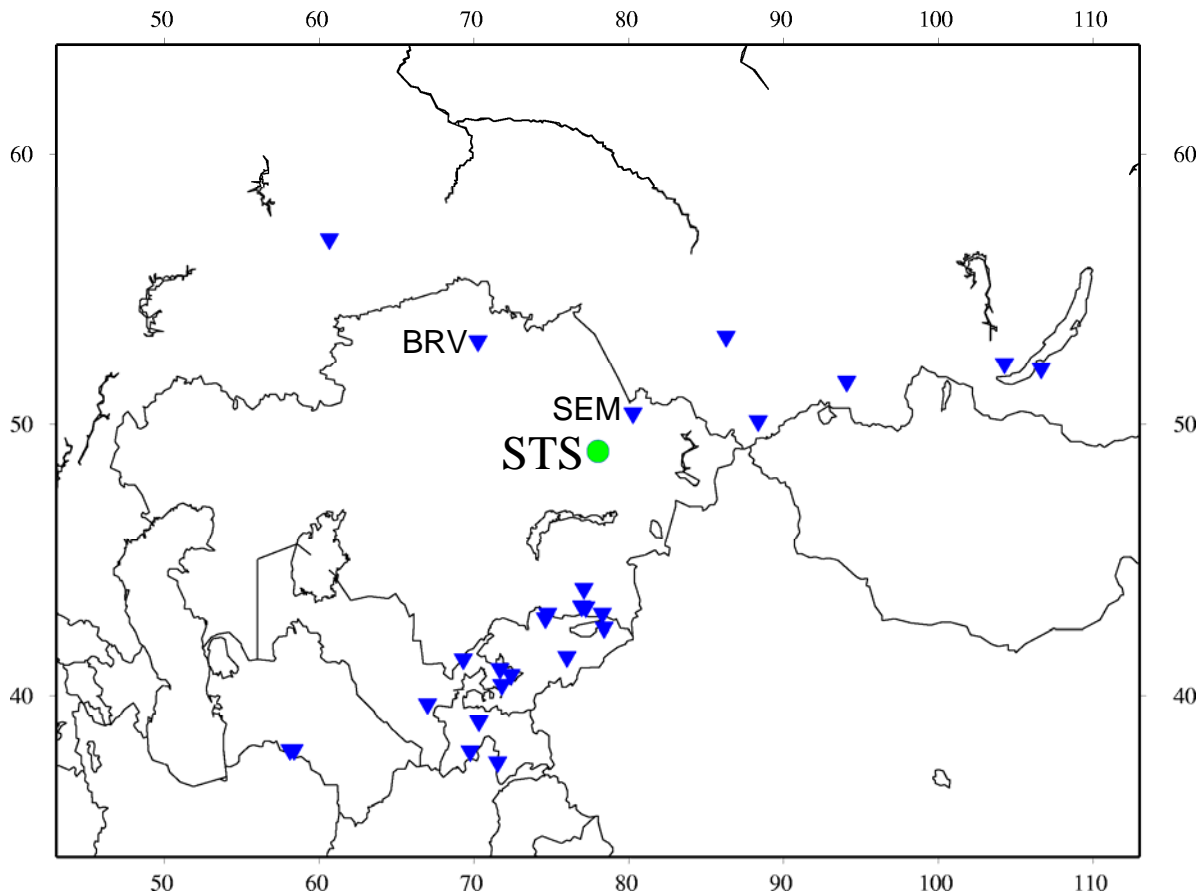


Figure 7. Distribution of seismic stations used in the analysis of seismic source scaling from the various regional phases observed from underground nuclear explosions at the former Soviet Semipalatinsk test site (STS). Labeled stations are those for which high resolution digital data are available.

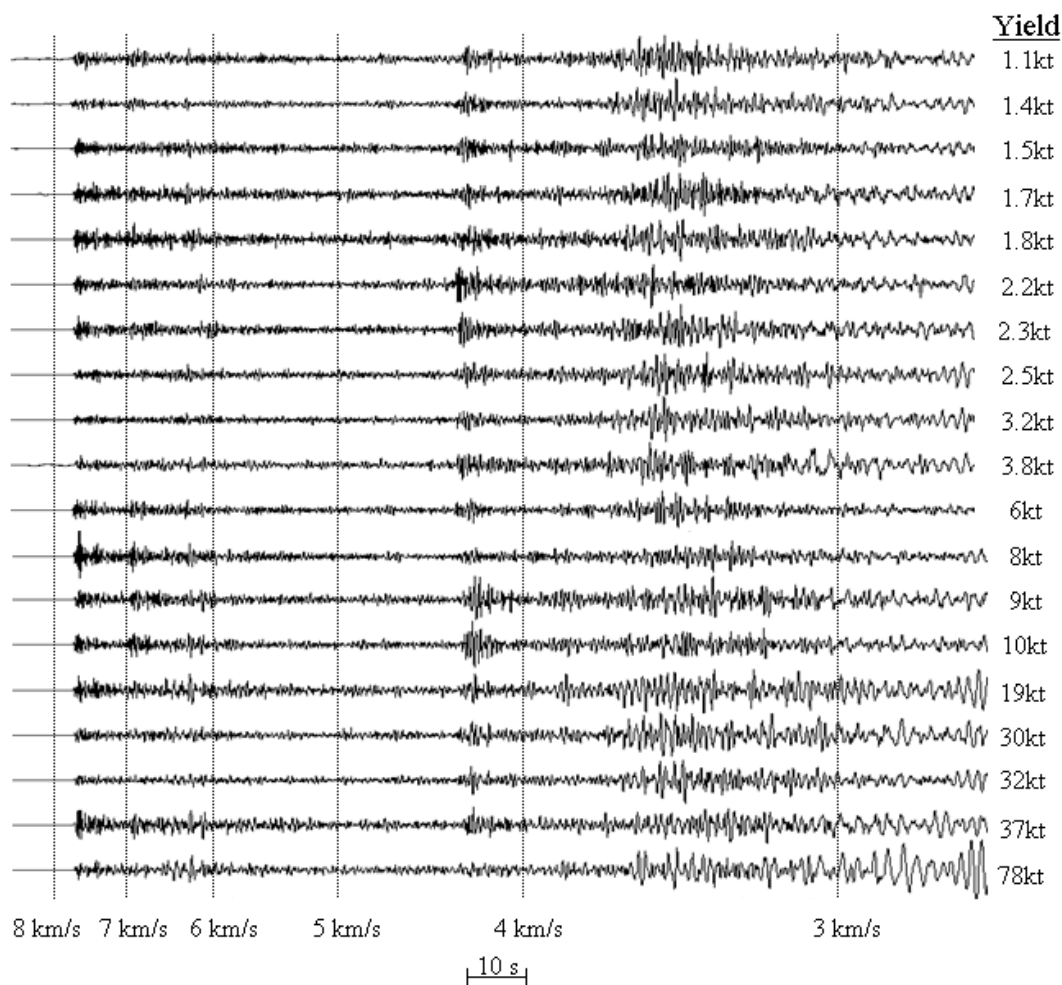


Figure 8. Vertical component digital data recorded at the Borovoye station (BRV, $\Delta \approx 650$ km) from a sample of Degelen Mountain nuclear explosions of known yield and depth of burial. The data are plotted as a function of apparent group velocity and in order of increasing yield between 1.1 and 78 kt.

available for the Balapan explosions. Vertical component data have been exclusively used throughout this study because they are generally of higher quality and more consistently available than the corresponding horizontal component data. Moreover, a number of previous studies have confirmed that horizontal component regional data from explosions scale with source size in essentially the same manner as the corresponding vertical component data (e.g. Murphy, 1977). In fact, averages of the spectral ratios on three component recordings are often used for discrimination purposes on the grounds that they are somewhat more stable than single component ratios. It can be seen from Figures 8 and 9 that if the Sn phase is associated with an apparent group velocity of about 4.5 km/sec and the Lg phase with an apparent group velocity of about 3.5 km/sec, then strong, broadband Sn and Lg arrivals are consistently observed at station BRV from explosions at both these testing areas.

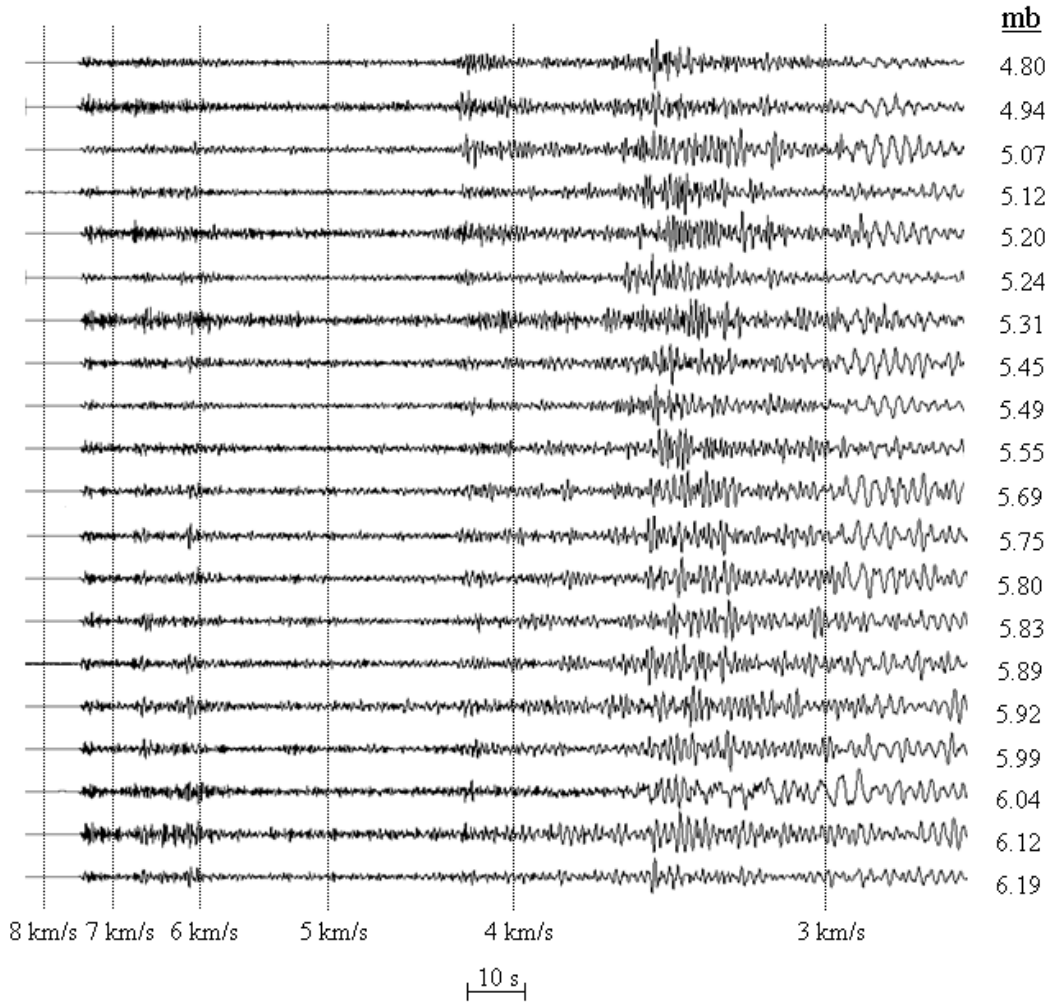


Figure 9. Vertical component digital data recorded at the Borovoye station (BRV, $\Delta \approx 650$ km) from a selected sample of Balapan explosions encompassing a range of m_b extending from 4.8 to 6.2. The data are plotted as a function of apparent group velocity.

While the Borovoye data are of generally good quality, close examination reveals numerous occurrences of spikes, data dropouts and clipping which would seriously contaminate any data analysis results at high frequency (Murphy et al, 2001). Consequently, all of the BRV data used in this study were carefully previewed by an experienced analyst to assess data quality and suitability for digital processing. In cases where such data problems were isolated as single points, they were corrected using simple interpolation of the adjacent data points, as is illustrated in Figure 10. In cases in which the data problems were too extensive to be remedied by such simple data interpolation, the recordings were deleted from the analysis data sample. The remaining, carefully previewed data were then processed to obtain regional phase spectral amplitude estimates using the narrowband filter processing described in Section 3.1 above. Figure 11 shows an example of the resulting filter outputs over the frequency range from 0.5 to

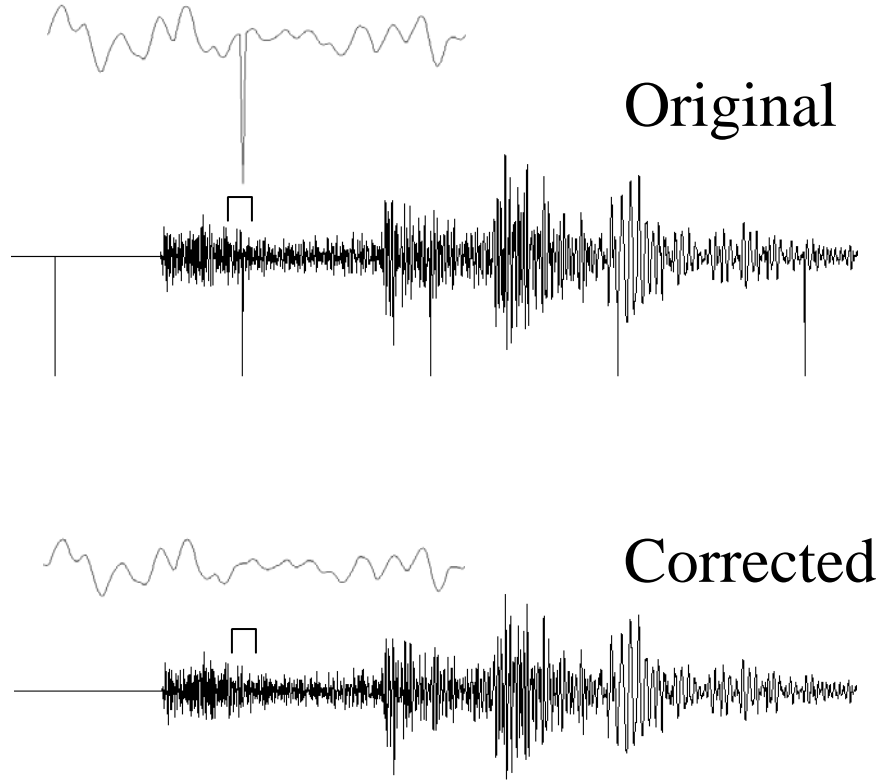
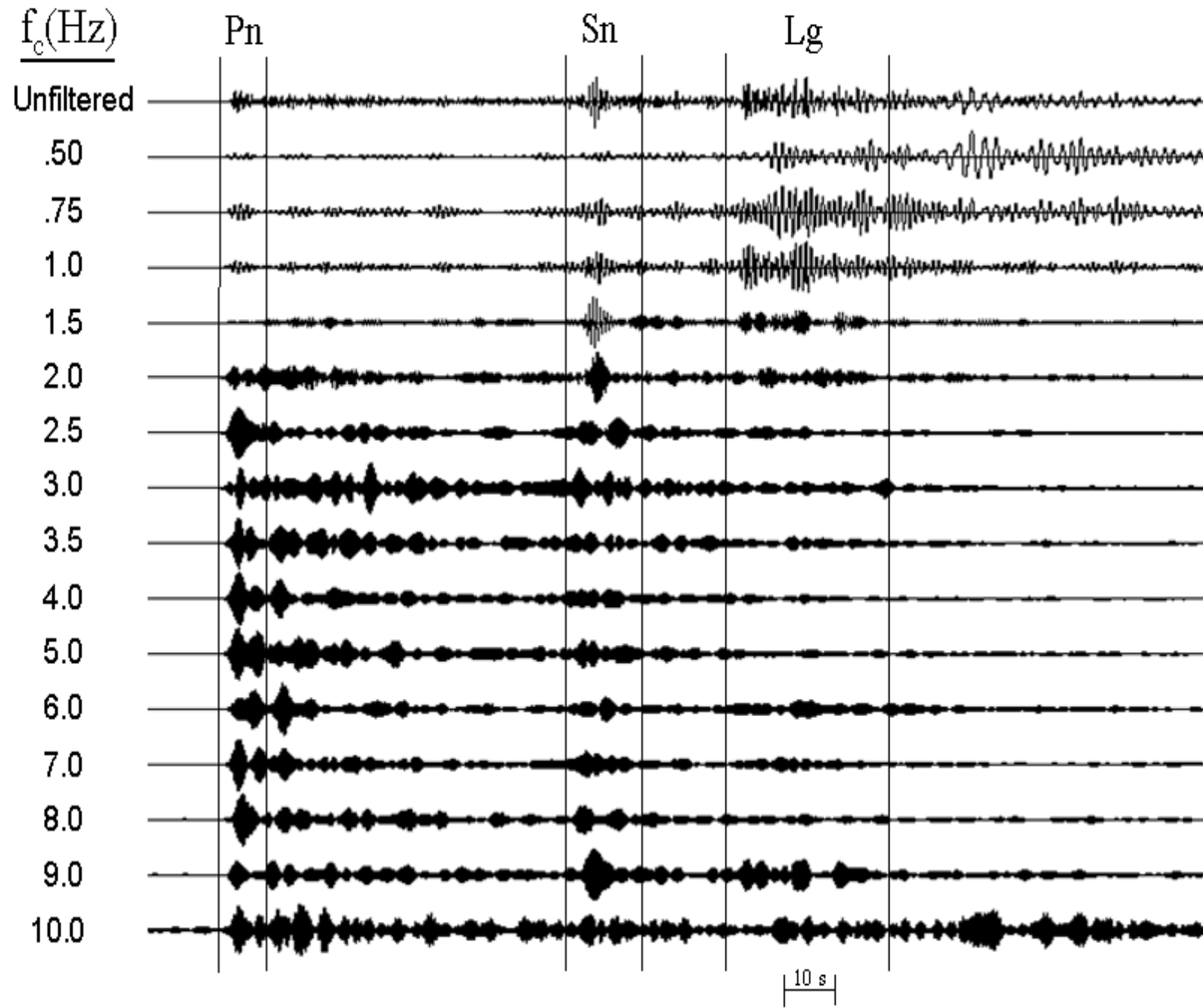


Figure 10. Example of a Borovoye explosion recording exhibiting numerous data spikes (top) and the same trace after processing it with a despiking routine (bottom).

10 Hz for the $m_b = 5.29$ Balapan explosion of 1 February 1979, where the selected time windows for the Pn, Sn and Lg phases are indicated. It can be seen that these filter outputs show large Lg/Pn amplitude ratios out to about 2 Hz, above which the Lg spectral amplitude level decreases quite rapidly to the P coda level at about 5 Hz. The observed Sn spectral amplitude levels are also greater than those of Pn out to about 3 Hz, but decrease less rapidly than those of Lg at higher frequencies, showing spectral amplitude levels above the P coda levels out to 10 Hz.

Before proceeding to the statistical analysis, it is instructive to directly compare observed regional phase spectral ratios corresponding to explosions with different sizes and depths of burial. Figure 12 shows a comparison of the station BRV Sn/Pn spectral ratios for Balapan explosions with m_b values of 4.94 and 6.19. Using the nominal average m_b /yield relation for Semipalatinsk explosions (Murphy and Barker, 2001), the yields of these two explosions differ by nearly a factor of 50, and it can be seen that their associated Sn/Pn spectral ratios are essentially identical over the entire frequency band extending from 0.5 to 10.0 Hz. This indicates that the observed Sn phase spectra must be scaling with yield in a very similar manner to the corresponding Pn phase spectra over this large range in explosion source size. Similarly, Figure 13 shows comparisons of observed station BRV Sn/Pn spectral ratios for selected Degelen explosions with



11. Bandpass filter processing results for the Borovoye recording of the $m_b = 5.29$ Balapan nuclear explosion of 2/01/79, where the selected time windows for the Pn, Sn and Lg regional phases are indicated.

significantly different depths and scaled depths of burial. It can be seen that these observed regional phase spectral ratios are also essentially identical over the sampled ranges of depth and scaled depth, consistent with a frequency dependent depth scaling for Sn which must be very similar to that for Pn, at least over the limited range of depths sampled by these Degelen explosions. It has been found that similar conclusions apply to the corresponding observed Lg/Pn spectral ratios. Thus, direct comparisons of observed data indicate that the Semipalatinsk Sn and Lg spectra from station BRV must be scaling with the explosion source variables in a manner which is very similar to that of the corresponding Pn spectra.

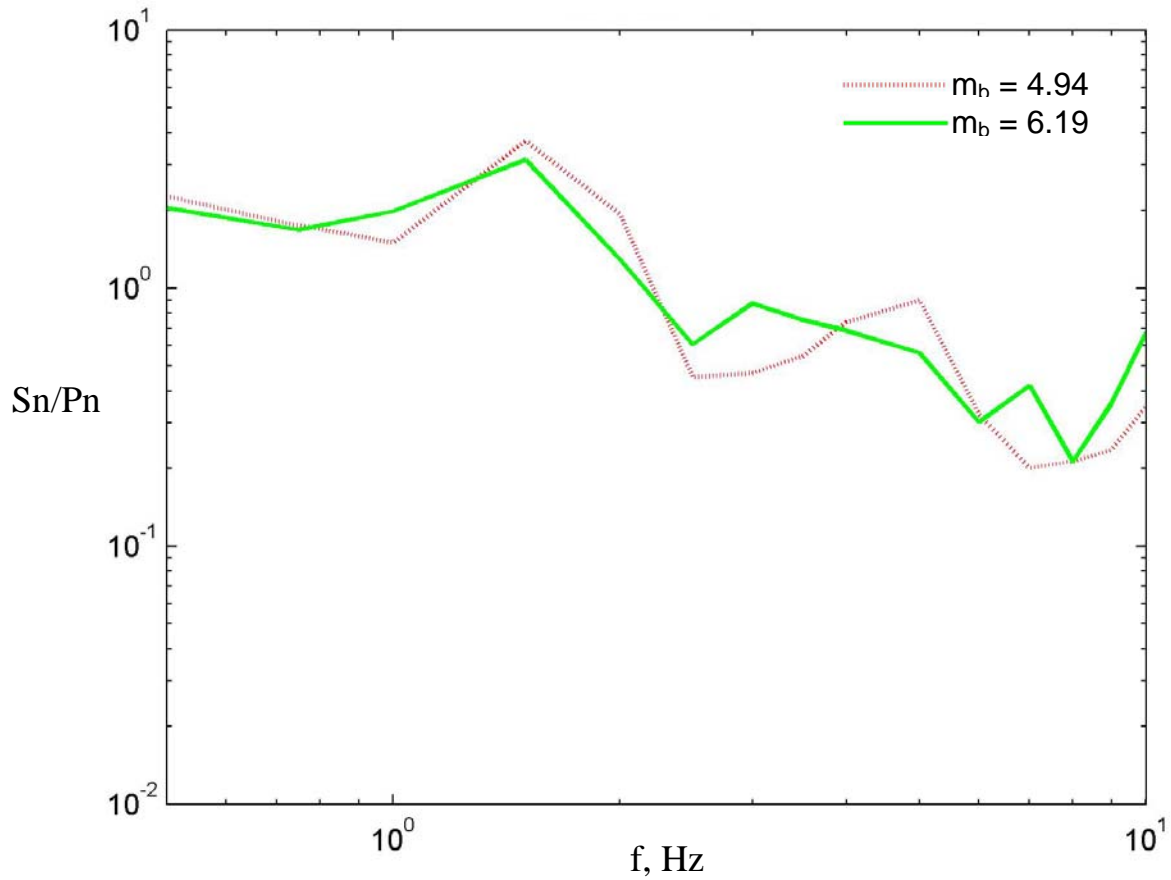


Figure 12. Comparison of observed Sn/Pn spectral ratios at station BRV for large and small Balapan explosions. These observed ratios are essentially identical, consistent with a frequency dependent magnitude scaling for Sn which must be very similar to that for Pn over this range of magnitude.

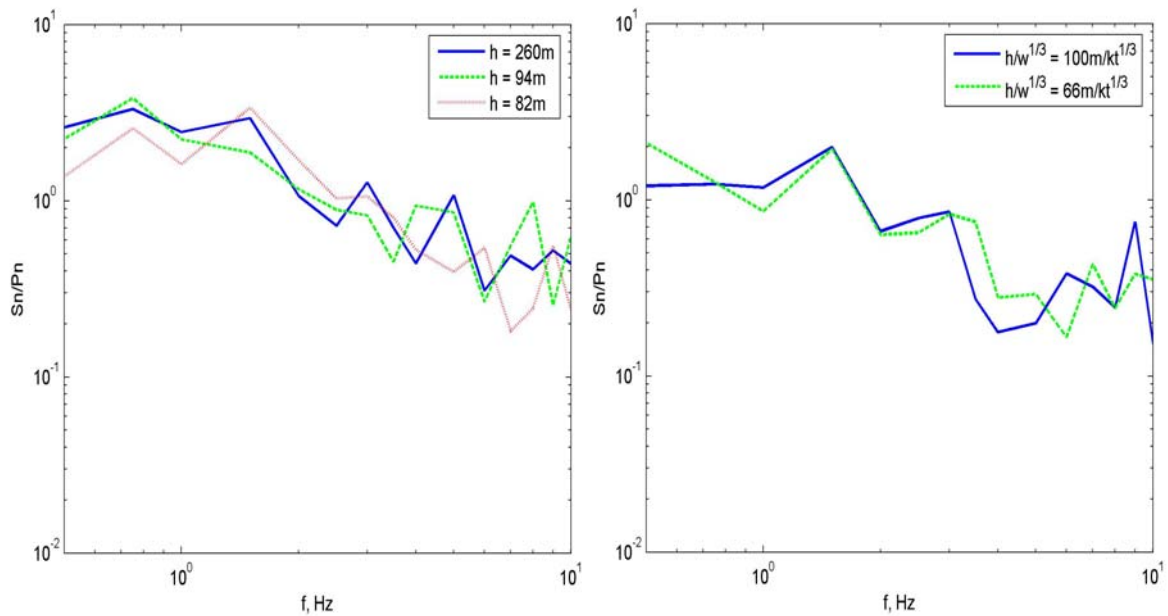


Figure 13. Comparison of observed Degelen Mountain Sn/Pn spectral ratios at station BRV as a function of source depth (left) and scaled depth (right).

The formal source scaling analysis was initiated with the regional phase amplitude data derived from the recordings of the 20 Degelen explosions of known yield shown in Figure 8, using the statistical model described in Section 3.1 above. The resulting yield scaling exponents for the regional phase spectral ratios S_n/P_n and L_g/P_n are displayed as functions of frequency in Figure 14, together with their observed associated 95% confidence bounds. As was noted previously, if the frequency dependent yield scaling for the secondary phases S_n and L_g is the same as that for P_n , then the scaling exponents for these ratios should not be significantly different from zero. In fact, the inferred scaling exponents are quite small, ranging only from about -0.25 to +0.10 over the frequency range from 0.5 to 10.0 Hz, and are significantly different from zero at the 95% confidence level only in a narrow band extending from about 1 to 3 Hz. That is, these statistical results also suggest that the observed S_n and L_g phase spectra scale with yield in a manner very similar to that for P_n , particularly in the higher frequency ranges used for regional discrimination purposes.

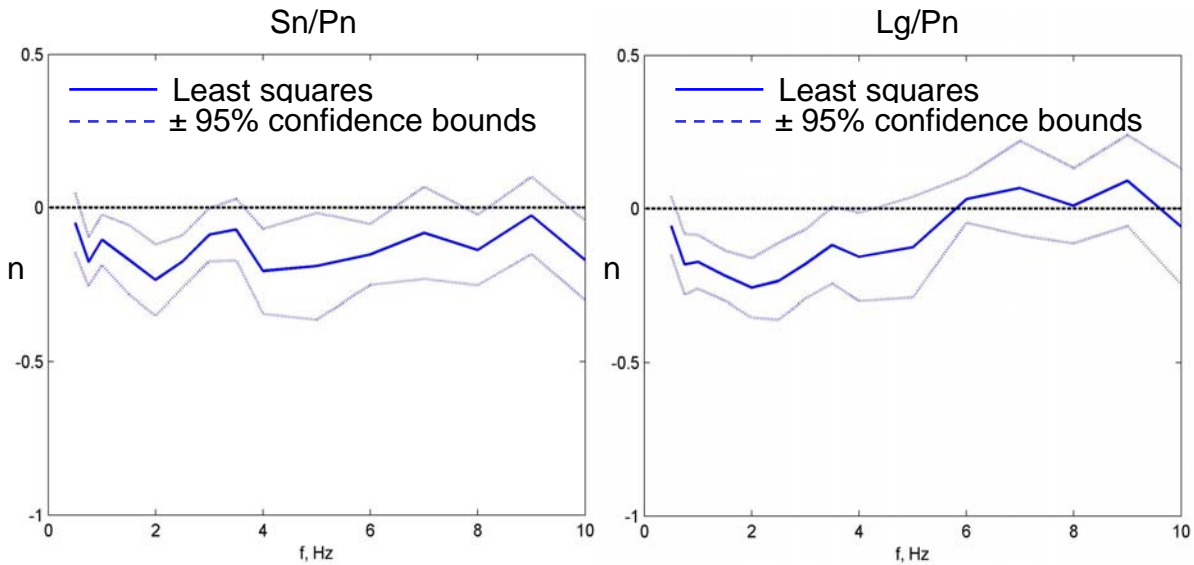


Figure 14. Estimated yield scaling exponents (n) as a function of frequency for the S_n/P_n (left) and L_g/P_n (right) regional phase spectral ratios at station BRV for Degelen Mountain explosions. It can be seen that these inferred yield scaling exponents are quite small, differing from zero at the 95% confidence level only in a narrow frequency range from about 1 to 3 Hz.

One limitation of the above analysis is that it is based on data recorded at a single station, and thus provides no insight into possible azimuthal variability of the source. For this reason, high resolution digital data recorded at near-regional station SEM, which is located at a significantly different azimuth (cf. Figure 7) have also been analyzed. Figure 15 (left) shows vertical component recordings from station SEM for four Degelen explosions with yields ranging from 1.5 to 90 kt. The right hand panel shows a comparison of the average S/P ratios for the two larger explosions ($\bar{W} = 58$ kt) with the

average S/P ratio for the two smaller explosions ($\bar{W} = 3.5\text{kt}$). It can be seen from this figure that these SEM S/P spectral ratios show no obvious yield dependence over the frequency range from 0.5 to 10 Hz, consistent with the corresponding station BRV results at a significantly different source to station azimuth.

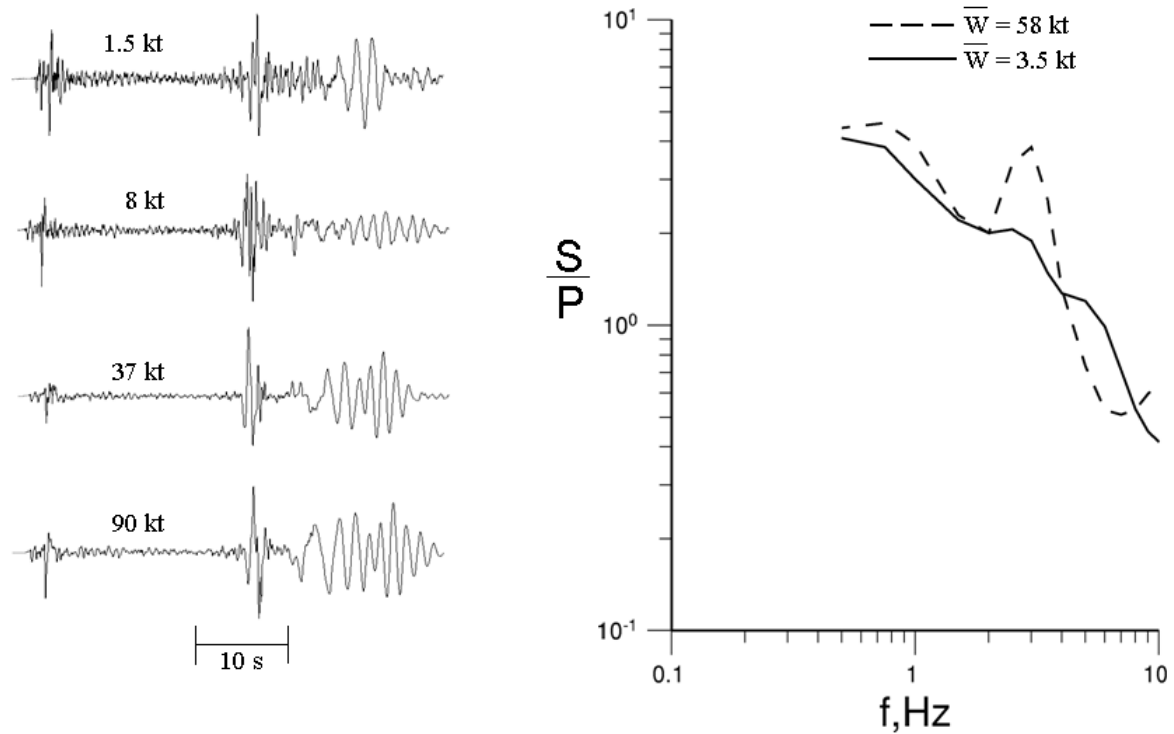


Figure 15. Comparison of vertical component seismic recordings (left) and associated average S/P spectral ratios (right) for selected Degelen Mountain explosions with yields ranging from 1.5 to 90 kt recorded at the near-regional ($\Delta \approx 175\text{ km}$) station SEM.

Additional evidence regarding azimuthal variability is provided by the regional phase peak amplitude data for Degelen explosions from the analog Soviet permanent network stations shown in Figure 7. While these data provide no information regarding possible frequency dependent variations, they do provide valuable constraints on possible azimuthal variations of the source in the short-period band. Figure 16 shows average Degelen explosion Sn/Pn and Lg/Pn peak amplitude ratios for some 25 of these Soviet network stations sampling a wide range of source to station azimuth. While the scatter is fairly large, these results indicate that any azimuthal variations in the seismic source functions of these regional phases must be small relative to the single station variability at a fixed azimuth, at least in the short-period band sampled by these data. Thus, the available data from these Degelen explosions provide no convincing evidence of any significant azimuthal dependence in the observed S/P phase amplitude ratios.

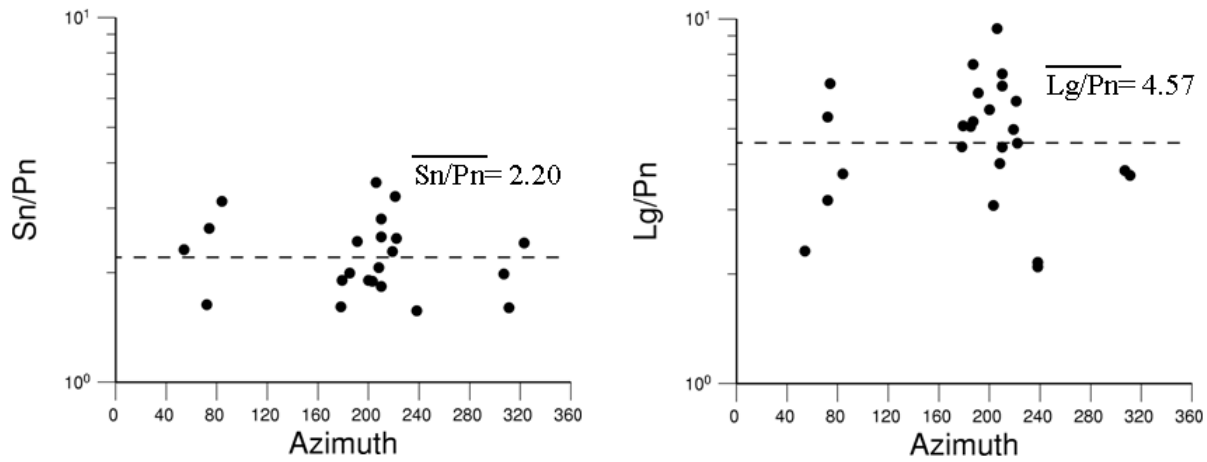


Figure 16. Average observed Degelen Mountain explosion Sn/Pn (left) and Lg/Pn (right) peak amplitude ratios as a function of source to station azimuth for Soviet permanent network stations.

Since both yield and m_b values are available for the 20 Degelen explosions of Figure 8, the regional phase spectral ratios derived from these station BRV data provide a good basis for testing the proposed alternate source scaling model in which m_b is used as a surrogate for yield, as described in Section 3.1 above. The two sets of frequency dependent yield scaling exponents derived from these Degelen Sn/Pn data are compared in Figure 17, where an average m_b /yield slope (i.e. b value) of 0.75 has been used to convert the m_b -based scaling exponents to yield scaling exponents in accord with the average Semipalatinsk m_b /yield relation inferred by Murphy and Barker (2001) from their analysis of observed network-averaged teleseismic P wave spectra from Semipalatinsk explosions. It can be seen that these two sets of inferred frequency dependent yield scaling exponents are very comparable, which supports the applicability of the m_b -based scaling model at testing areas such as Balapan and Lop Nor where yields of significant numbers of individual explosions are not known.

For the Balapan analysis, a sample of station BRV recordings from about 60 explosions encompassing a range of m_b extending from about 4.8 to 6.2 were assembled and carefully previewed to assure data quality. These data were then processed to obtain Sn/Pn and Lg/Pn spectral ratios, which were then statistically analyzed to determine frequency dependent yield scaling exponents using the procedures described in Section 3.1. The resulting Balapan yield scaling exponents are plotted as functions of frequency for Sn/Pn and Lg/Pn in Figure 18, where they are compared with corresponding Degelen results from Figure 14. It can be seen from this figure that the estimated yield scaling exponents for these two Semipalatinsk testing areas are very similar, with the Balapan exponents also being significantly different from zero only in the narrow frequency band between about 1 and 3 Hz. Also shown on this figure are the corresponding theoretical

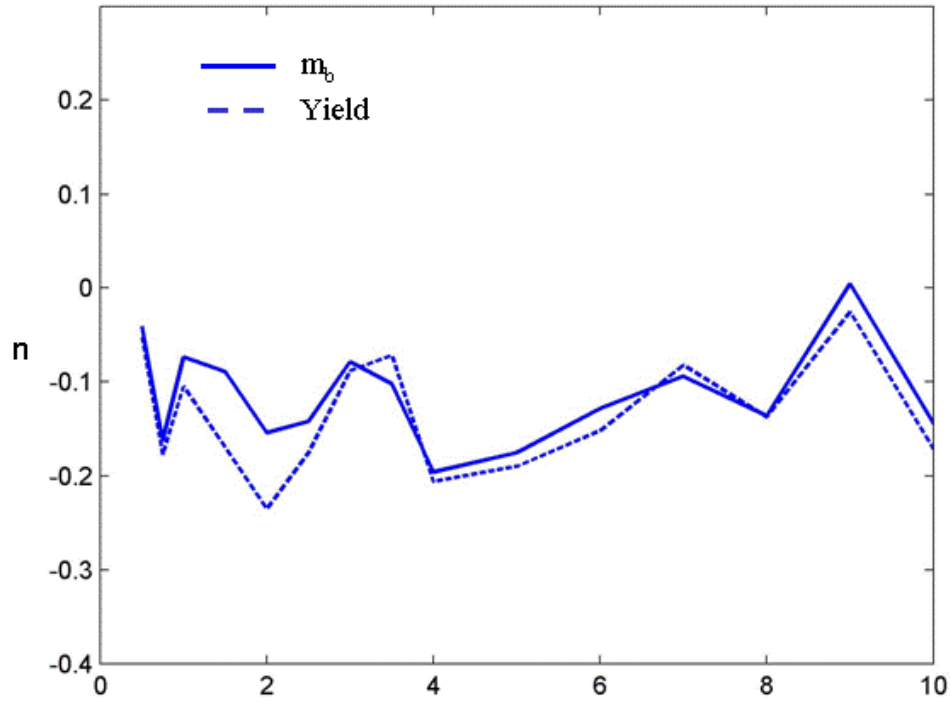


Figure 17. Comparison of frequency dependent yield scaling exponents (n) for the Degelen Sn/Pn Borovoye spectral ratios estimated from regressions with respect to yield (dashed) and m_b (solid).

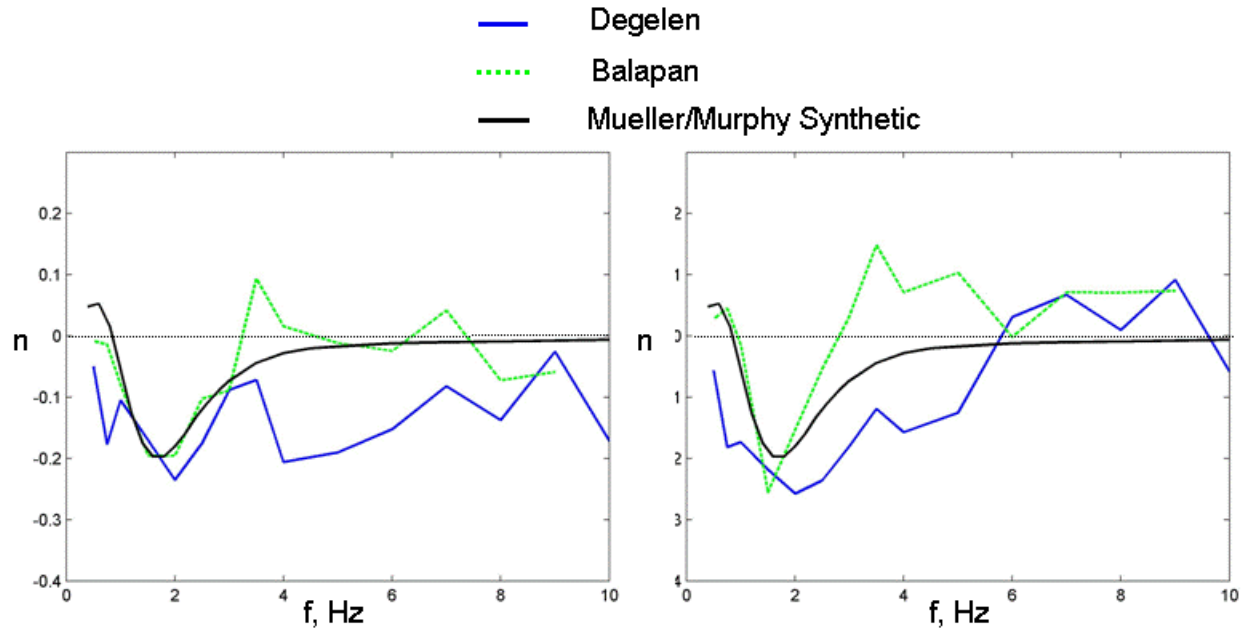


Figure 18. Comparison of observed Degelen and Balapan frequency dependent yield scaling exponents for Sn/Pn (left) and Lg/Pn (right) with the theoretical exponents predicted by a simple source model based on Mueller/Murphy, with $S_n(f) = P_n(kf)$, where k represents the ratio of the P to S wave velocities of the source medium.

frequency dependent yield scaling exponents predicted for these sets of explosions using the simple phenomenological source model described in Section 3.2 above, in which the S wave source is estimated from the corresponding Mueller/Murphy P wave source by scaling the corner frequency by the S/P velocity ratio of the source medium. It can be seen that these theoretical yield scaling exponents as a function of frequency are remarkably consistent with the experimental Semipalatinsk values, within the approximate ± 0.1 uncertainty bounds on these statistically inferred values.

Given the success of the simple Mueller/Murphy based phenomenological model in explaining the observed frequency dependence of the source scaling of the Semipalatinsk S/P spectral ratios, it remains to identify plausible physical sources which are consistent with this model. Now, since the source corner frequency in the Mueller/Murphy P wave model is proportional to the compressional wave velocity divided by the elastic radius, it follows from the comparisons shown in Figure 18 that the S wave sources for these explosions must have characteristic lengths comparable to those of the corresponding P wave sources. One physical mechanism for S wave generation that would be consistent with this inference is the tectonic model proposed by Archambeau (1972) and Stevens (1980), in which an explosion in a prestressed medium causes a stress release in the nonlinear zone surrounding the explosion in which the medium is crushed and cracked by the outgoing compressional shock wave out to a range approximately equal to the elastic radius characteristic of the P wave source. If such a mechanism is in fact responsible for S wave generation by explosions, then it would be expected that the observed S/P ratios would depend on the strength of the individual explosion-induced tectonic release in some systematic fashion. However, for explosions at Balapan where the strength of the long-period tectonic release was very precisely estimated for a large number of events by Given and Mellman (1986), there does not appear to be any obvious correlation of the observed S/P spectral ratios with the corresponding inferred tectonic release. This fact is illustrated in Figure 19, where the Borovoye Sn/Pn spectral ratios for two Balapan explosions having very similar m_b values but very different long-period tectonic release characteristics (as measured by the F factor which is equal to the inferred ratio of the moment of the equivalent tectonic release double couple to the moment of the explosion source) are compared. It can be seen that these two spectral ratios are essentially identical over the 0.5 to 10.0 Hz frequency band, indicating that the S wave generation efficiency in this band does not correlate with the strength of the accompanying tectonic release, at least as measured by the long-period F factor. Thus, the search continues for a plausible physical mechanism for S wave generation by explosions which is consistent with the inferred source scaling characteristics of the observed S/P spectral ratios.

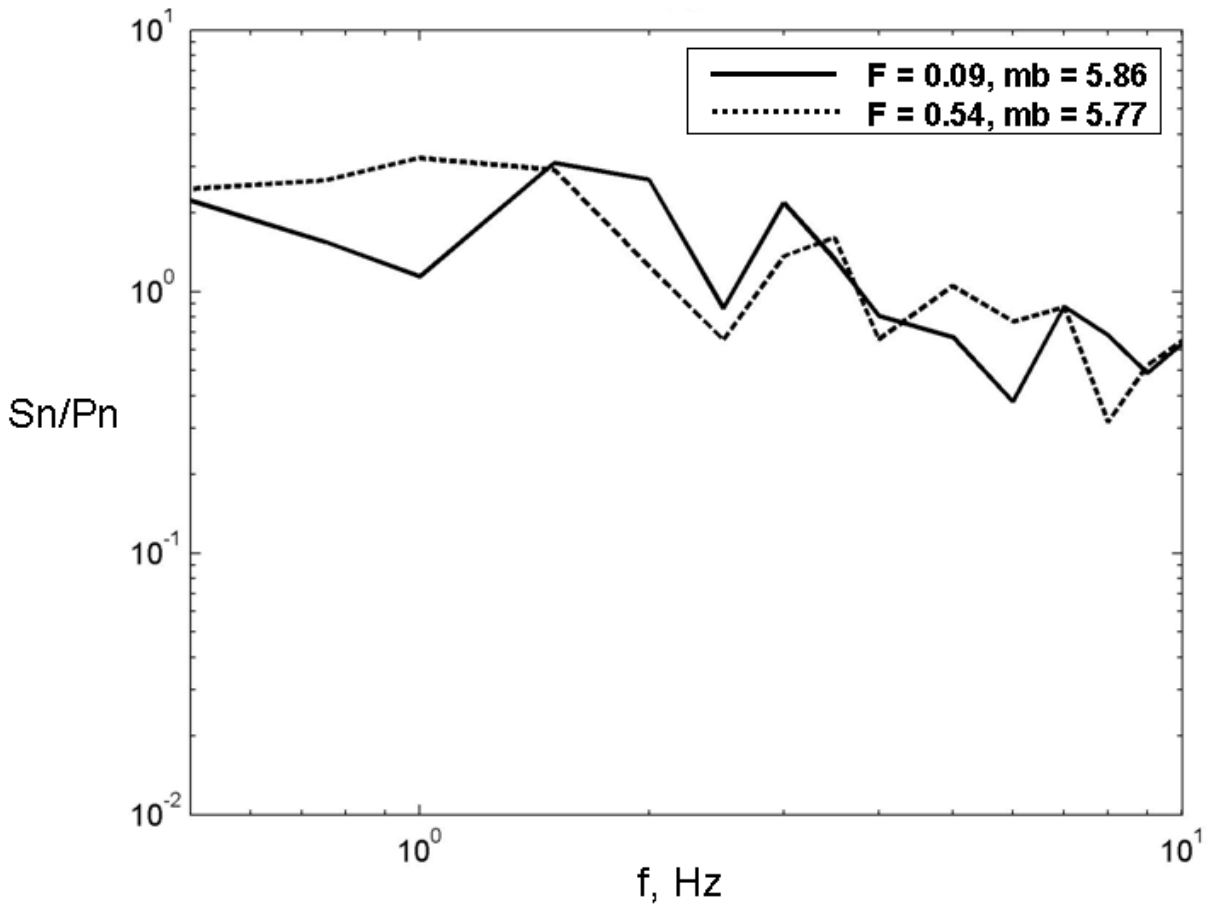


Figure 19. Comparison of observed Sn/Pn spectral ratios for two Balapan explosions of comparable yield, but significantly different long-period tectonic release characteristics (i.e. F factors). It can be seen that these observed spectral ratios show no statistically significant dependence on F in the 0.5 to 10 Hz frequency band.

4.2 Lop Nor

The map locations of the digital stations for which data have been assembled for a sample of Lop Nor nuclear explosions encompassing a range of m_b extending from 4.8 to 6.6 are shown in Figure 20. It can be seen that, although there are no data useful for source scaling analyses available from stations in China, there are numerous stations located near the border within the territories of the former Soviet Union, including station MAK that is located at a comparable distance from Lop Nor (i.e. $\Delta = 7^\circ$) to that of the Borovoye station from the Semipalatinsk test site.

An example of representative bandpass filtering processing results for the assembled sample of Lop Nor data is shown in Figure 21 for the station AAK ($\Delta = 10^\circ$) recording of the Lop Nor explosion of 29 July 1996. This example is typical in that, unlike the Borovoye recordings of Semipalatinsk explosions, there is no obvious Sn arrival which can be correlated across the frequency range of interest. Moreover,

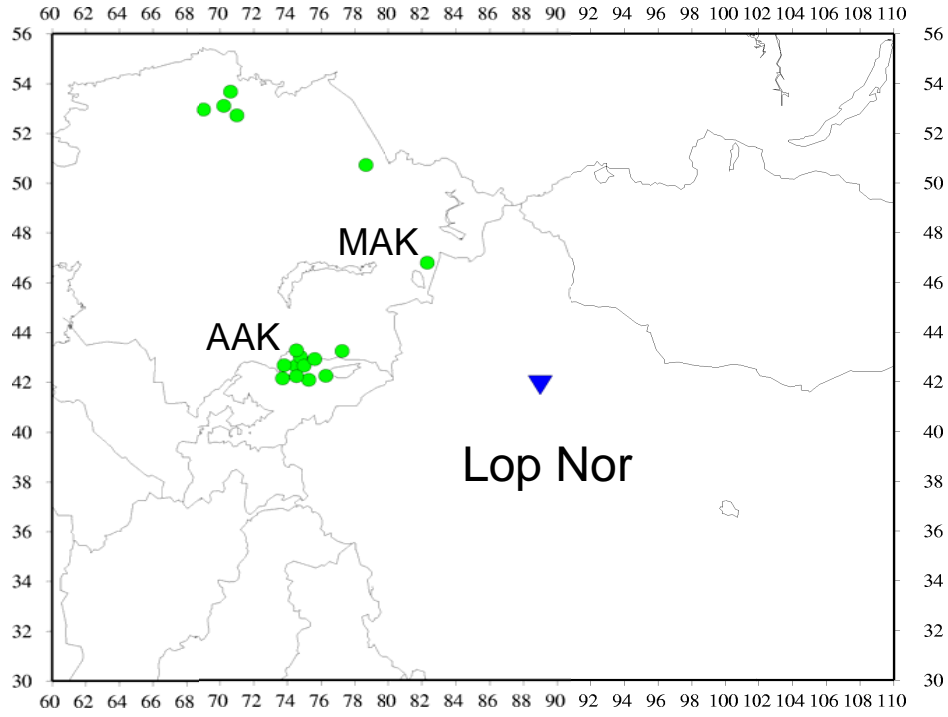


Figure 20. Distribution of digital seismic stations used in the analysis of seismic source scaling of regional phases from Lop Nor explosions.

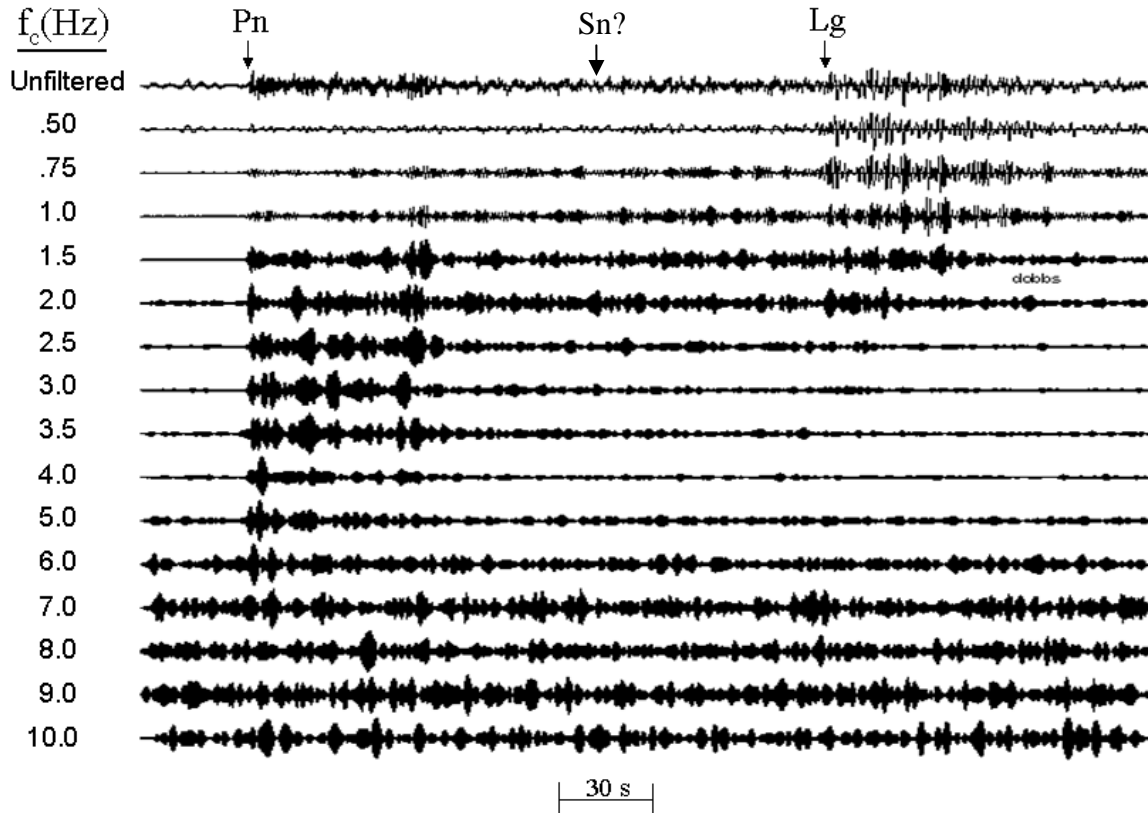


Figure 21. Bandpass filter processing results for the station AAK ($\Delta=10^\circ$) recording of the Lop Nor explosion of 29 July 1996.

although the Lg phase is observed to be relatively strong at low frequencies, its amplitude level decreases quite rapidly to the P coda level above about 3 Hz. Although these results vary somewhat from station to station, there is no evidence of Lg energy above the P coda level at frequencies above 5 Hz at any of these stations. Consequently the Lop Nor source scaling analysis has been limited to the Lg/Pn spectral ratios at frequencies below 5 Hz.

As in the Semipalatinsk analyses, it is instructive to directly compare observed regional phase spectral ratios at common stations for Lop Nor explosions of different sizes before proceeding to the formal statistical analysis. Figure 22 shows a comparison of observed station MAK ($\Delta = 7^\circ$) Lg/Pn spectral ratios estimated from recordings of four Lop Nor explosions encompassing a range of m_b extending from 4.8 to 5.8. Based on the nominal average m_b /yield relation for Lop Nor explosions (Murphy and Barker, 2001), this range in m_b corresponds to more than a factor of 20 in yield (i.e. $b = 0.75$), and it can be seen that the associated Lg/Pn spectral ratios are very similar over the frequency range extending from 0.5 to 5.0 Hz. That is, as at Semipalatinsk, these Lop Nor Lg source spectra must be scaling with yield in a very similar manner to that of the corresponding Pn source spectra over this range in explosion source size.

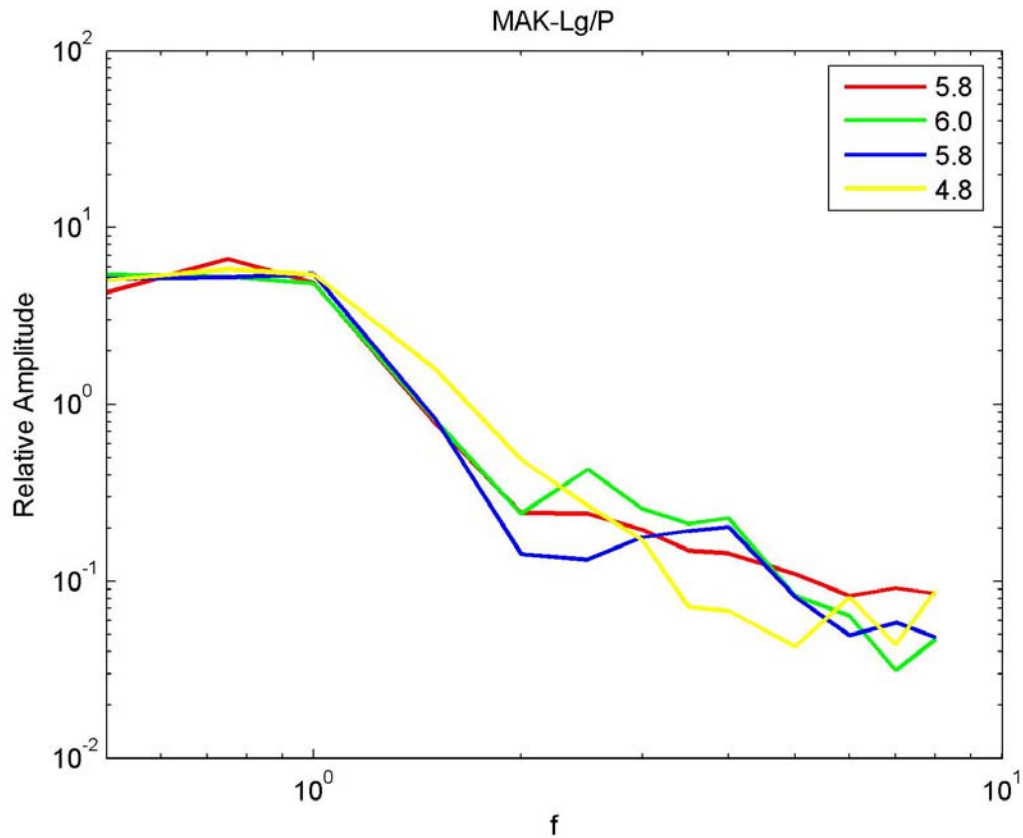


Figure 22. Comparison of observed Lg/Pn spectral ratios at station MAK ($\Delta = 7^\circ$) for Lop Nor explosions encompassing a wide range of source size.

Although digital data are available from Lop Nor explosions at a number of different stations (cf. Figure 20), unlike Semipalatinsk there is no one station that recorded explosions sampling the entire range of energy release encompassed by the explosions represented in our Lop Nor database. Consequently, for this test site a modified covariance statistical approach was applied to the source scaling analysis of the observed Lg/Pn spectral ratio data. In this model, the Lg/Pn spectral ratio at station i from explosion j is represented in the form

$$\left(\frac{\text{Lg}}{\text{Pn}} \right)_{ij} = K_i(\omega) W_j^{n'(\omega)} \quad (12)$$

where the frequency dependent yield scaling exponent, $n'(\omega)$, is assumed to be common to all stations, and the $K_i(\omega)$ are the frequency dependent station terms which are estimated statistically using samples of observed Lg/Pn spectral ratio data from explosions of known yield (or, in this case, known m_b) at the various stations. The applicability of this selected technique is illustrated in Figure 23 which shows observed Lg/Pn ratios from the various stations at a frequency of 1.5 Hz for a sample of Lop Nor explosions encompassing a range of m_b extending from 4.8 to 6.6. The left panel of this figure shows the raw Lg/Pn amplitude ratio data from the various stations plotted as a function of m_b , while the right panel shows the corresponding station-corrected values. It can be seen that the inferred station corrections significantly reduce the interstation data scatter, permitting a confident determination of the source scaling exponent. The Lg/Pn frequency dependent yield scaling exponents estimated from the Lop Nor explosion data are shown in Figure 24 where they are compared with the corresponding Balapan exponents over the frequency range extending from 0.5 to 5.0 Hz. It can be seen that these Lop Nor source scaling results are remarkably similar to those for Balapan, again indicating that the difference in yield scaling exponents between the S and P wave sources are significantly different from zero only in a narrow band from about 1 to 2 Hz. As at Semipalatinsk, these observed Lop Nor S/P spectral ratios have been theoretically simulated using the simple Mueller/Murphy based S wave source model, and the frequency dependent yield scaling exponents derived from these synthetic ratios are compared with those estimated from the observed Lop Nor Lg/Pn ratios in Figure 25. Once again, the agreement is excellent, indicating that the observed Lop Nor source scaling for Lg/Pn is also consistent with a simple S wave source which is directly related to the corresponding P wave source.

4.3 Novaya Zemlya

Assembling a suitable database for source scaling analysis of regional S/P spectral ratios for Novaya Zemlya explosions proved to be difficult because, while a number of regional digital stations in the area have recorded some of the explosions conducted at that test site, the only station which operated continuously for a long enough period of time to record data from Novaya Zemlya explosions sampling a wide range of yields in NORSAR. However, because NORSAR is located at a far-regional distance of nearly 20° from these explosions, the observed S wave spectral amplitudes generally exceed the corresponding P coda amplitude levels only for frequencies below about 2 Hz. Consequently, the most that can be concluded from these data is that the observed S/P

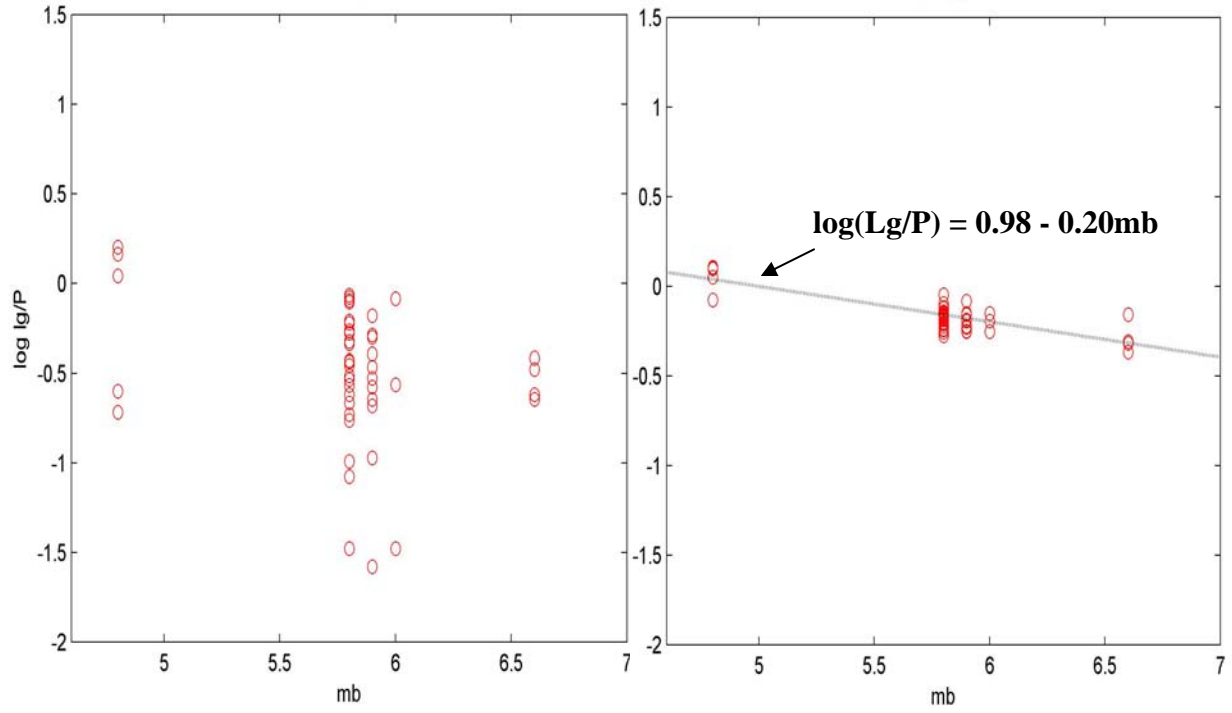


Figure 23. Comparison of Lop Nor Lg/Pn spectral ratios as a function of m_b at 1.5 Hz. The left panel shows the measured phase spectral ratio values from the various stations while the right panel shows the corresponding station-corrected phase spectral ratio values obtained from the covariance analysis.

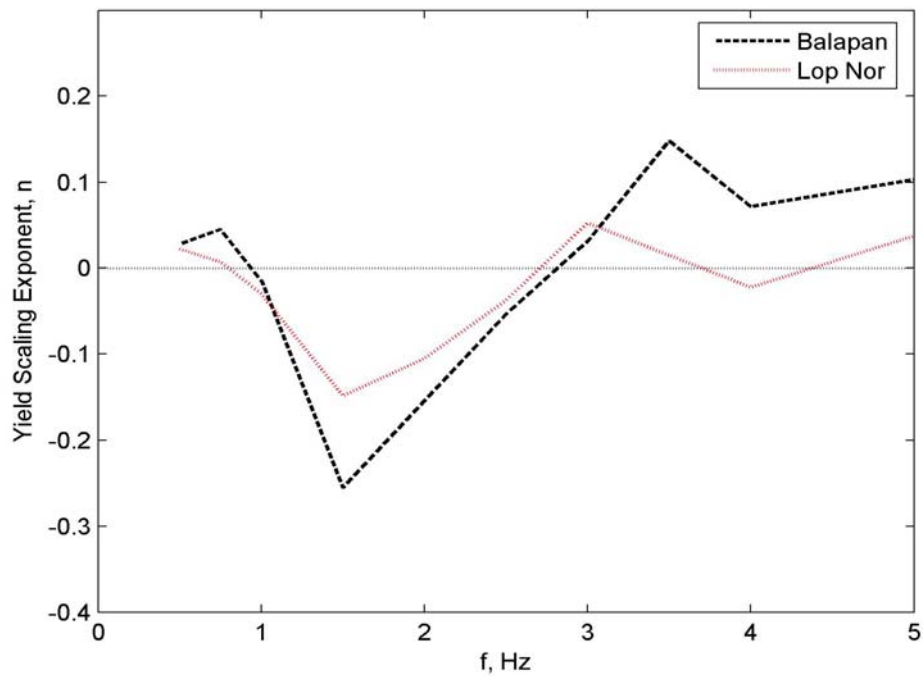


Figure 24. Comparison of observed Lop Nor and Balapan frequency dependent yield scaling exponents for Lg/Pn.

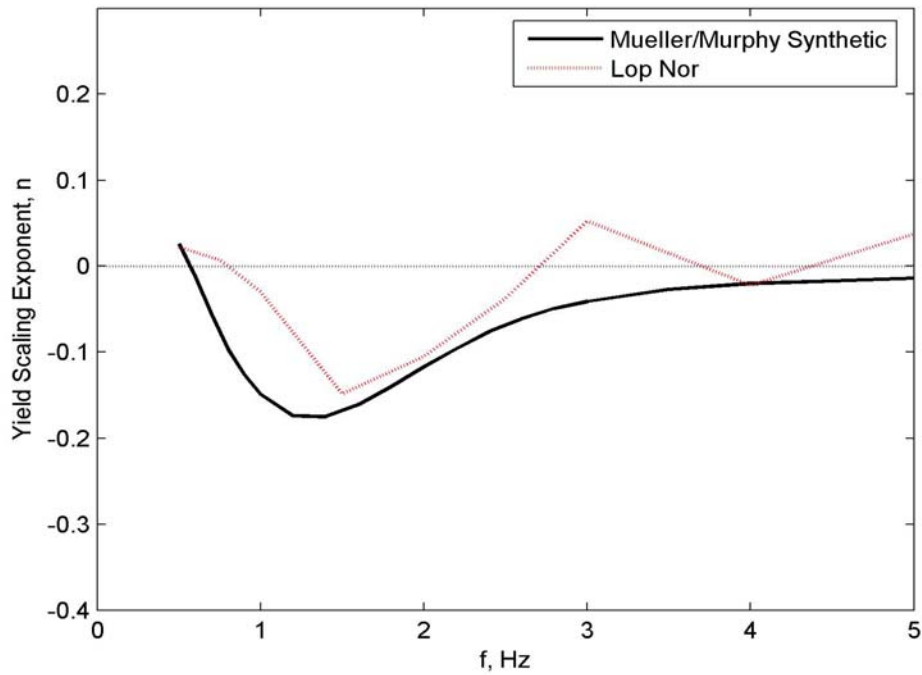


Figure 25. Comparison of observed Lop Nor frequency dependent yield scaling exponents for Lg/Pn with the theoretical exponents predicted by a simple source model based on Mueller/Murphy, with $S(f) = P(kf)$ where k represents the ratio of the P to S wave velocities of the source medium.

spectral ratios appear to be roughly independent of source size over the limited frequency band extending from about 0.5 to 2.0 Hz, consistent with the previously described results for explosions at the Semipalatinsk and Lop Nor test sites.

In an attempt to derive more definitive results, the study effort was redirected to an analysis of the yield dependence of observed Novaya Zemlya explosion S/P spectral ratios derived from data recorded at the four Russian special monitoring regional stations whose map locations are shown in Figure 26. Although only limited samples of Novaya Zemlya explosion data are currently available from these stations, their proximity to the testing areas enables analysis of S/P yield dependence at frequencies up to about 5 Hz, which is difficult using data recorded at the more distant Scandinavian stations.

The most suitable data for purposes of the present analysis that are currently available from these special monitoring stations are recordings of the same two Southern Novaya explosions of very different size at the near-regional Amderma and Nar-yan-Mar stations. The Amderma vertical component recordings from these two explosions are shown in Figure 27. Based on the nominal average m_b /yield relation for Novaya Zemlya (Murphy and Barker, 2001), these two explosions differ in yield by about a factor of 30, and it can be seen that this difference in yield is evident in the recordings in that the

dominant frequencies of the various arrivals are significantly lower for the larger $m_b = 7.0$ explosion of 10/27/73 than for the smaller $m_b = 5.9$ explosion of 9/27/73. Despite these obvious differences in source corner frequency, it has been found that the S/P spectral ratios for these two explosions are very similar at both stations. This fact is illustrated for the Sn/Pn spectral ratios in Figure 28, where it can be seen that the observed ratios for the two explosions are essentially identical over the frequency range from 0.5 to 5.0 Hz at both stations. Similar conclusions apply to the corresponding Lg/Pn spectral ratios. Thus, while these data are not extensive enough to permit a formal statistical scaling analysis, they are consistent with the results presented above for explosions at the Semipalatinsk and Lop Nor test sites in that they show no significant dependence of the regional phase S/P spectral ratios on explosion yield.

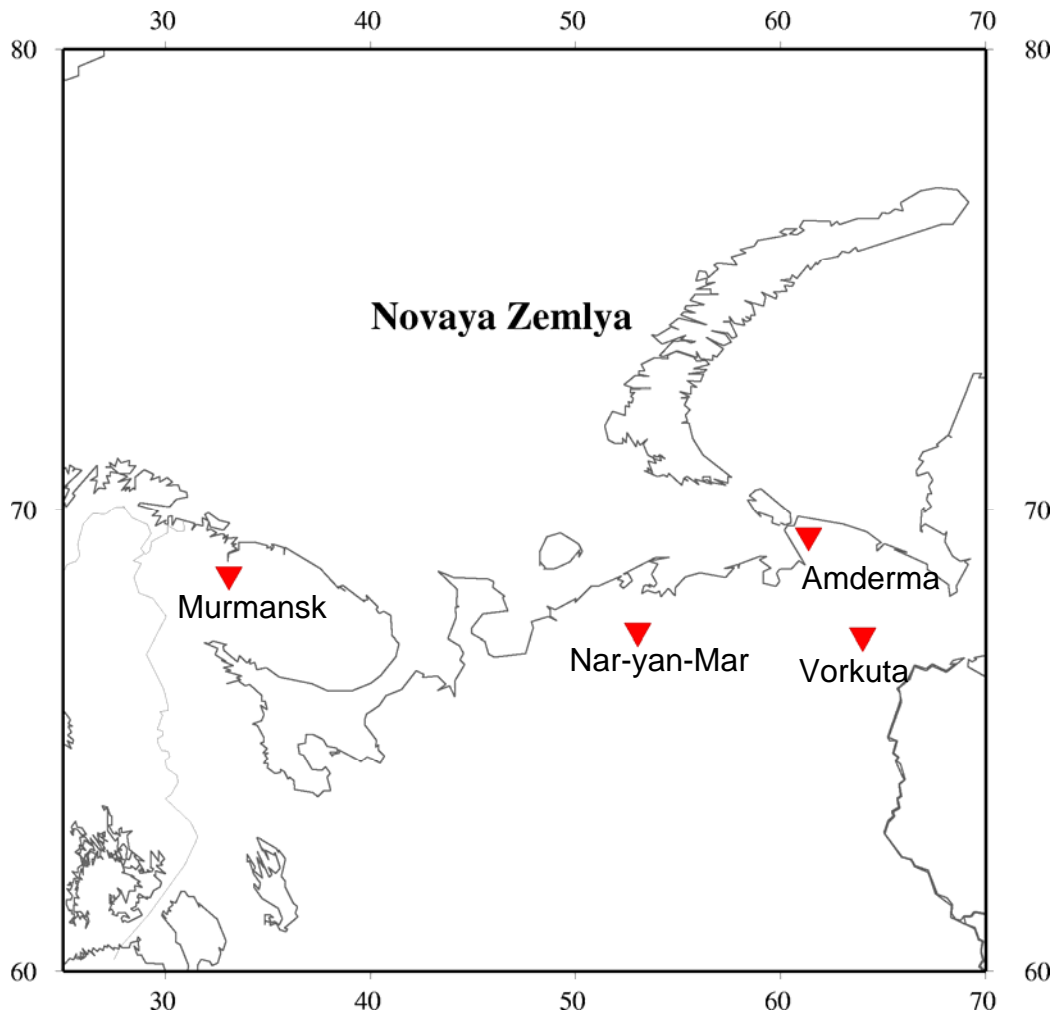


Figure 26. Near-regional Russian seismic stations for which high resolution digital data are available for selected Novaya Zemlya explosions.

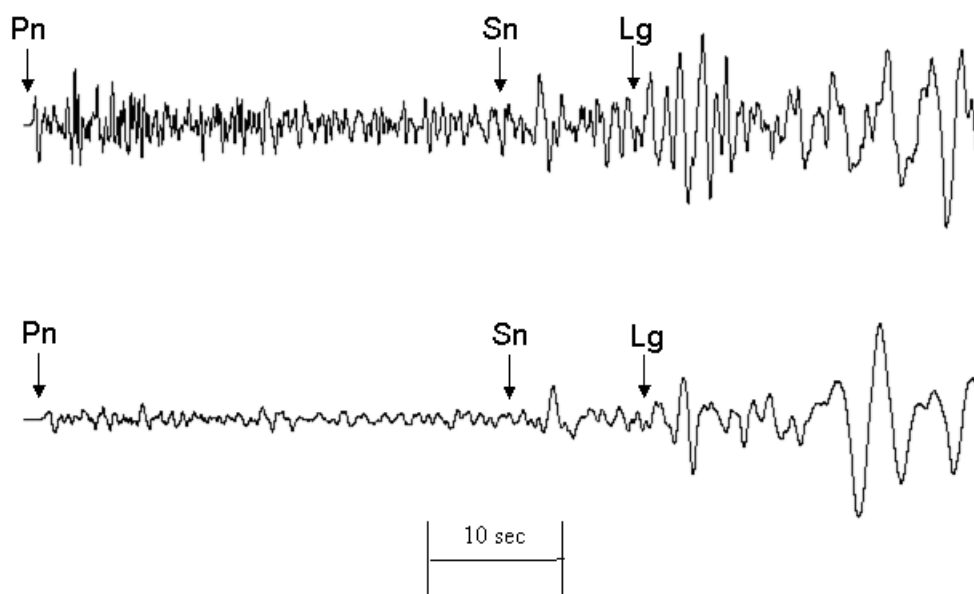


Figure 27. Comparison of vertical component recordings of the Southern Novaya Zemlya explosions of 9/27/73 ($m_b = 5.9$, top) and 10/27/73 ($m_b = 7.0$, bottom) at near-regional station Amderma ($\Delta \approx 320$ km).

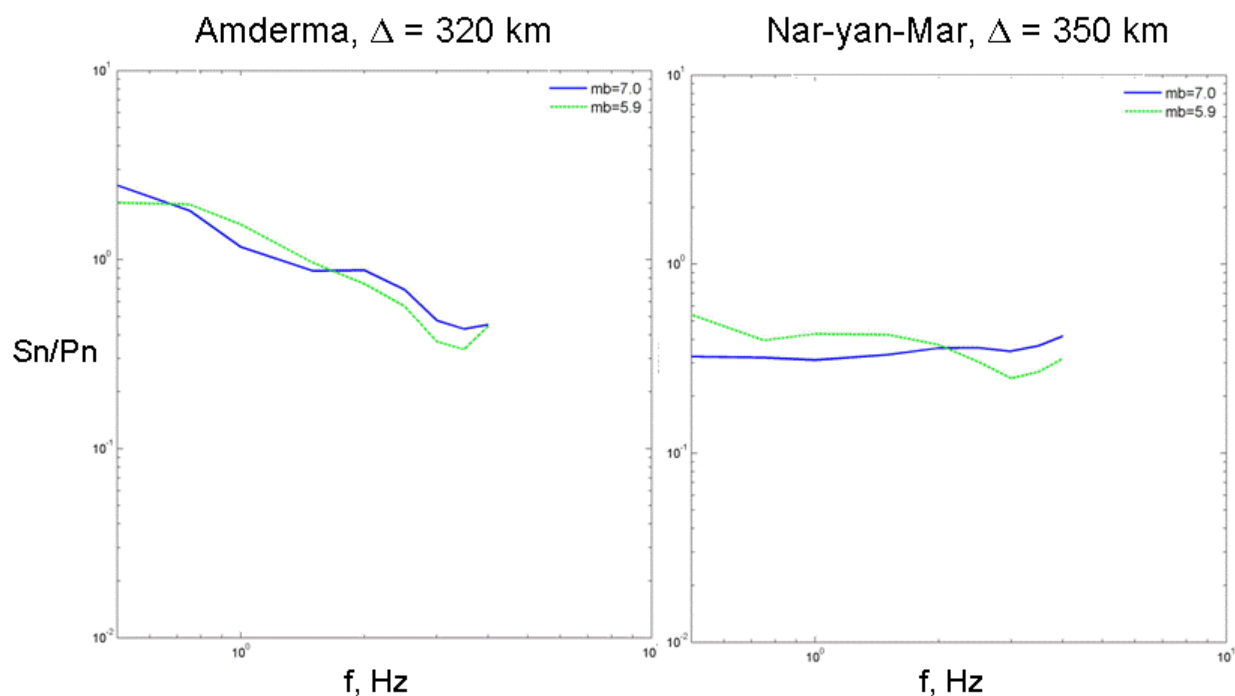


Figure 28. Comparison of Sn/Pn spectral ratios for Southern Novaya Zemlya explosions of 9/27/73 ($m_b = 5.9$) and 10/27/73 ($m_b = 7.0$) at stations Amderma (left) and Nar-yan-Mar (right).

4.4 NTS

The S/P scaling analysis for the NTS test site has focused on data recorded at the four near-regional Lawrence Livermore National Laboratory (LLNL) seismic network stations from explosions conducted below the water table at the Yucca Flat testing area. The map locations of these four stations with respect to the Yucca Flat testing area on NTS are shown in Figure 29 where it can be seen that they are well situated to detect any azimuthally dependent variations in the seismic sources of the regional phases of interest. This restricted source region was selected to minimize effects due to variations in source coupling and propagation paths for the different explosions. Figure 30 shows a sample of vertical component recordings at LLNL station MNV (Mina, Nevada) at an epicentral distance of about 240 km from selected explosions detonated below the water table at Yucca Flat. It can be seen that these explosions encompass a range of m_b extending from 4.1 to 5.9 that, according to the average nominal m_b /yield relation for well-coupled explosions at NTS (Murphy, 1981; 1996), corresponds to a seismic yield range extending from about 1 to 200 kt. Thus, these data provide a good basis for assessing effects of explosion source size on the observed S/P spectral ratios. It can be seen from this figure that even the smallest of these explosions is recorded at good signal to noise ratios at this near-regional station. Representative bandpass filter outputs obtained from processing the explosion Techado recording at station MNV are displayed in Figure 31. Note that the spectral amplitude levels of S exceed the corresponding P coda levels up to frequencies on the order of 10 Hz in this near-regional distance range.

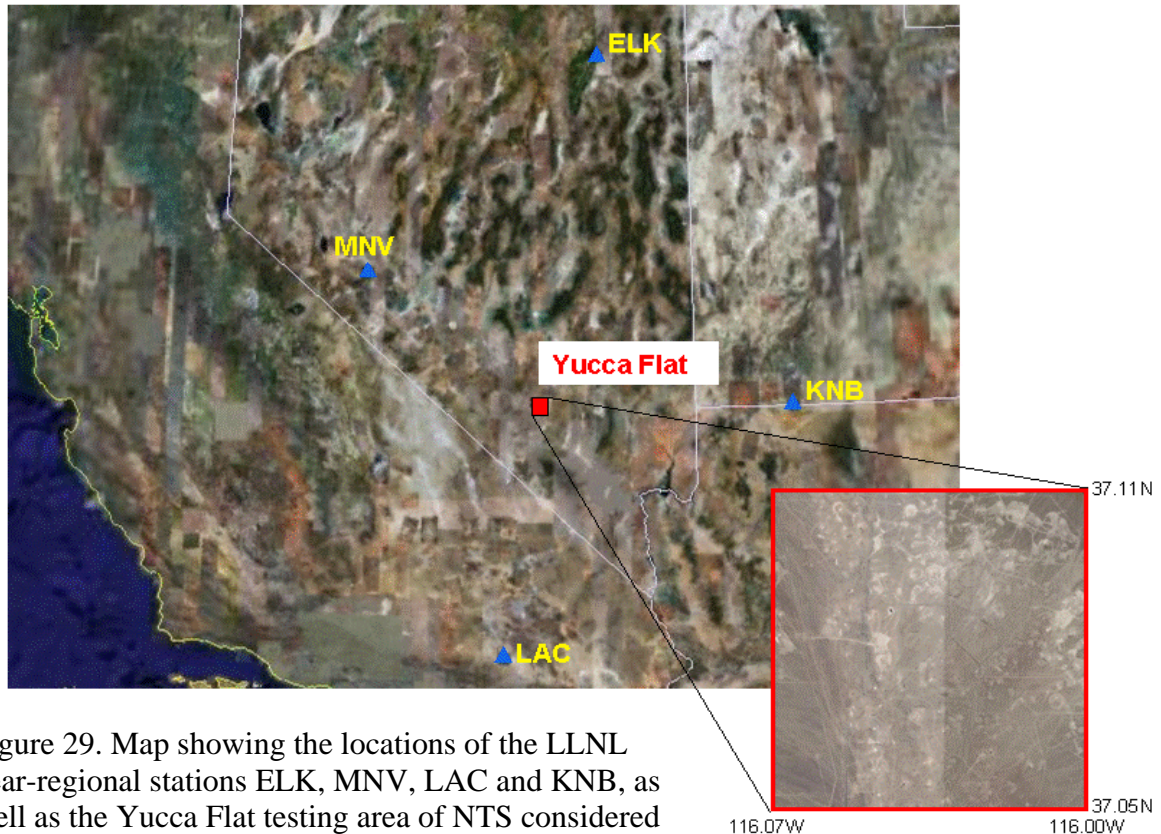


Figure 29. Map showing the locations of the LLNL near-regional stations ELK, MNV, LAC and KNB, as well as the Yucca Flat testing area of NTS considered in the present study.

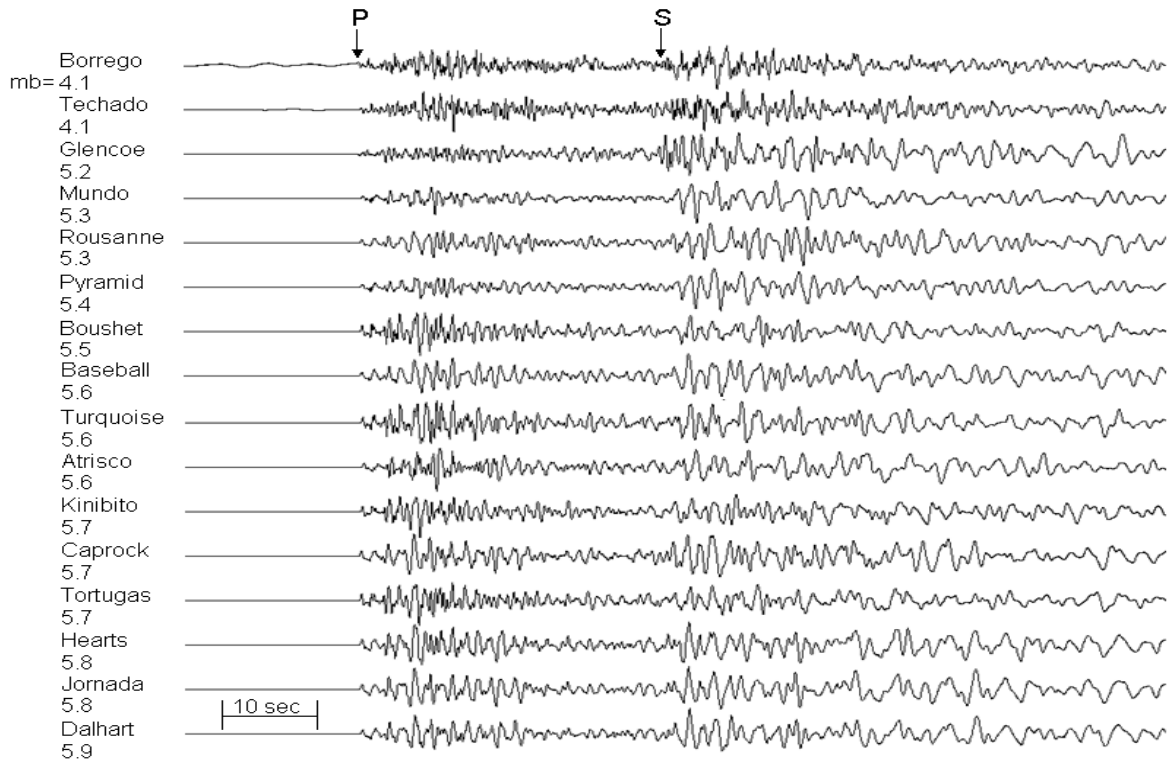


Figure 30. Vertical component digital data recorded at the Mina, Nevada LLNL network station (MNV, $\Delta \approx 240\text{km}$) from a selected sample of explosions detonated below the water table at Yucca Flat which encompass a range of m_b extending from 4.1 to 5.9.

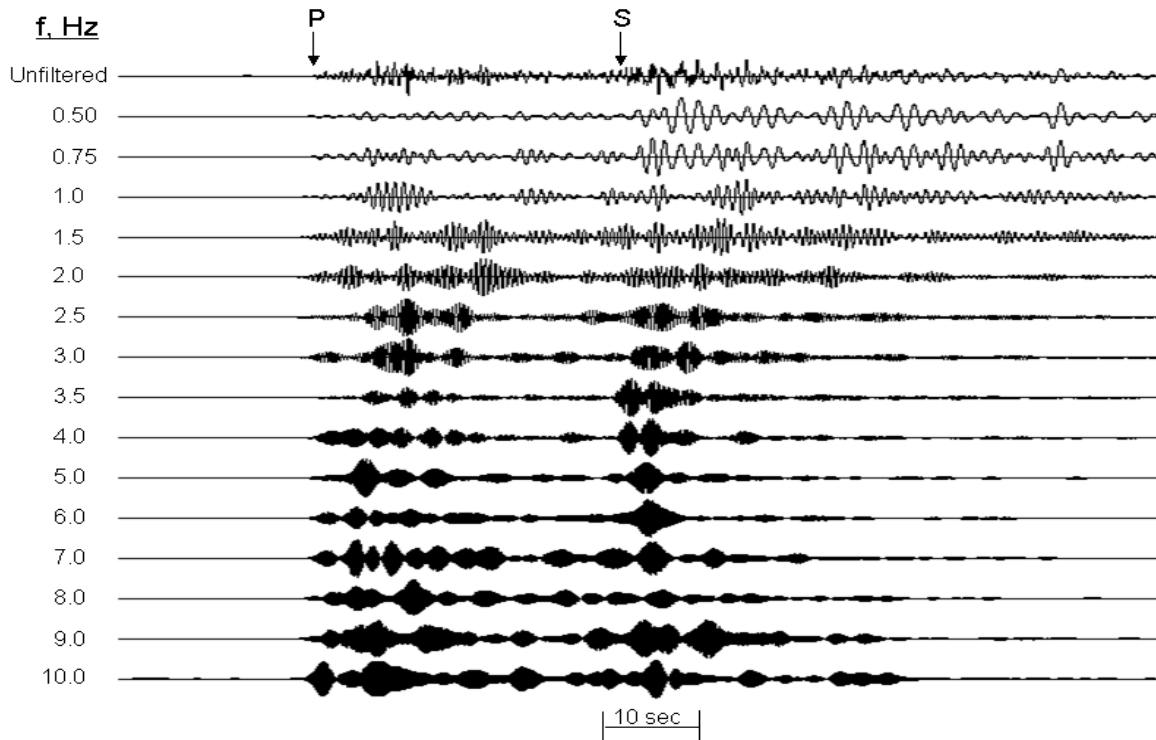


Figure 31. Bandpass filter processing of the LLNL station MNV recording of the NTS explosion Techado ($m_b = 4.1$). It can be seen that the S wave spectral amplitude levels are above the P coda levels out to 10 Hz.

Many of the Yucca Flat explosions in the selected data set were recorded at all four of the LLNL stations and, consequently, the following analysis will focus on network-averaged (logarithmic) S/P spectral ratios, since these appear to be somewhat more stable than the corresponding single station values. Figure 32 shows a comparison of such network-averaged S/P spectral ratios for seven Yucca Flat explosions sampling a range in m_b extending from 4.1 to 5.9. It can be seen that, while the results for the different explosions are generally quite consistent, there is a tendency for the S/P ratios for the smallest explosions (i.e. Tehcado, Borrego) to lie somewhat above those for the larger explosions (i.e. Baseball, Scantling, Sandreef, Caprock, Dalhart) over a fairly broad frequency range between about 0.5 and 5.0 Hz. An even more dramatic example is provided in Figure 33 which shows a comparison of S/P spectral ratios at LLNL station LAC (Landers, California) for the very small ($M_L = 3.5$) Aleman and much larger ($m_b = 5.8$) Caprock explosions. It can be seen from this figure that the S/P spectral ratio for the smaller Aleman explosion is significantly larger than that for the larger Caprock explosion over the frequency band from about 0.5 to 5.0 Hz, in apparent contradiction of the results described above for the other three test sites.

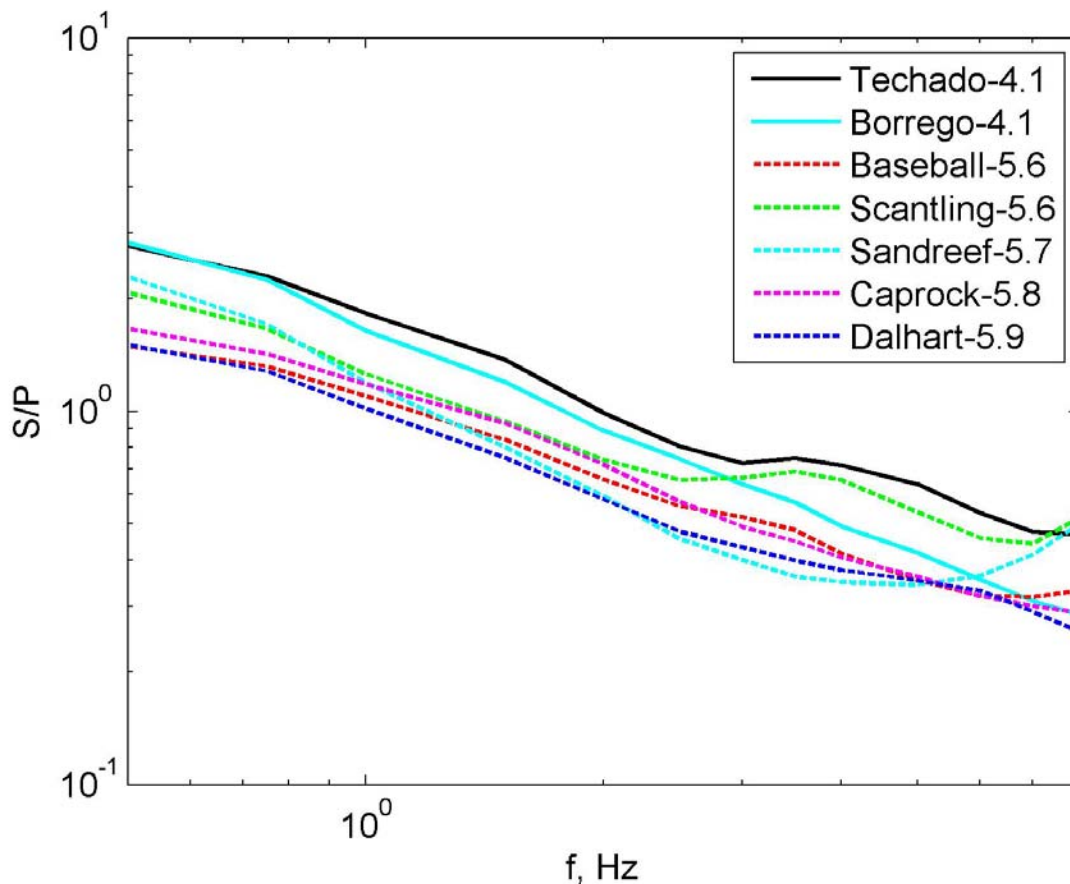


Figure 32. Comparison of LLNL network average S/P spectral ratios for selected explosions conducted below the water table at Yucca Flat. Solid lines denote the ratios corresponding to the smallest explosions (Tehcado, Borrego) while dashed lines denote the ratios corresponding to the larger explosions (Baseball, Scantling, Sandreef, Caprock, Dalhart).

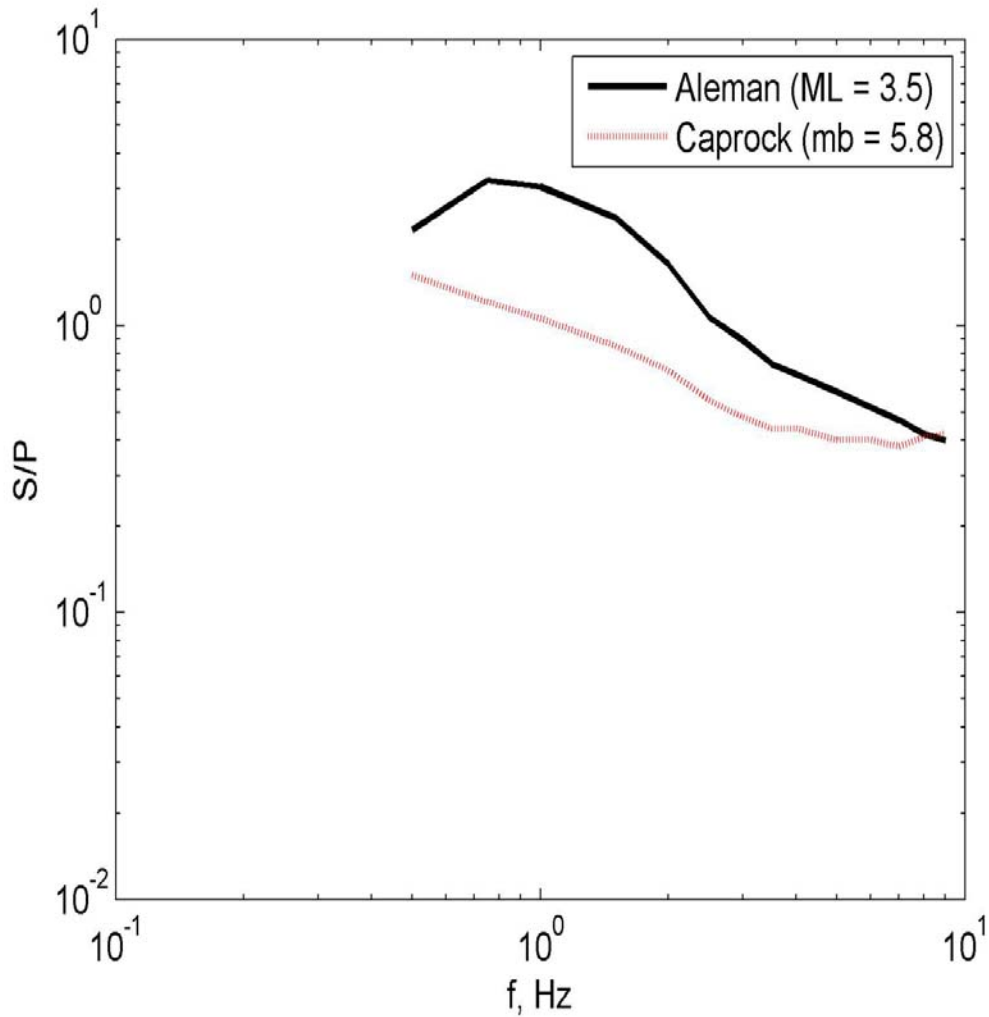


Figure 33. Comparison of S/P spectral ratios estimated from LLNL station LAC recordings of small (Aleman) and large (Caprock) Yucca Flat explosions.

In fact, however, more detailed investigation has revealed that these observations are also consistent with the simple Mueller/Murphy based model for S/P. That is, because of the sampling constraint that all the selected explosions should have been detonated below the water table, these low yield explosions were all conducted at depths of more than 500m, which is four to five times deeper than the nominal scaled depth for containment of about $122W^{1/2}$. It follows that, since the Mueller/Murphy model predicts that the source corner frequency will increase with increasing depth as $h^{0.42}$, the expected corner frequencies for these overburied, low yield explosions are about a factor of two higher than those expected for the same yield explosions at nominal containment depths. The net result is that S/P ratios predicted by the Mueller/Murphy based model for the selected set of NTS explosions shows a significant yield dependence over a large portion of the frequency range of interest. This fact is illustrated in Figure 34 which shows a comparison of the theoretical S/P spectral ratios predicted by the Mueller/Murphy based

model for an explosion in saturated tuff with a yield of 1 kt and a depth of burial of 550m and an explosion with a yield of 150 kt and a depth of burial of 650m. It can be seen that the theoretical S/P ratios corresponding to these two sets of source conditions differ appreciably over the frequency band extending from about 0.5 to 5 Hz. The degree to which this model fits the observed Yucca Flat S/P spectral ratios is illustrated in Figure 35 which shows a comparison of the ratio of the observed Aleman S/P ratio to the average observed S/P ratio for five Yucca Flat explosions having a mean m_b value of about 5.7 with the corresponding theoretical ratio predicted by the Mueller/Murphy based model. It can be seen that the simple phenomenological model fits the observed S/P ratio data almost exactly. The corresponding average spectral ratio obtained using observed S/P values from the three smallest explosions in the selected sample (i.e. Aleman, Techado, Borrego) is shown in Figure 36, where it is again compared with the corresponding Mueller/Murphy based model prediction. It can be seen that, although the agreement with the corresponding theoretical ratio is not as precise in this case as that obtained with Aleman alone, it is still well within observational uncertainty, and this provides some very strong constraints on allowable S wave generation mechanisms for these NTS explosions, particularly in view of the fact that the smaller explosions were so deeply overburied relative to normal containment depths.

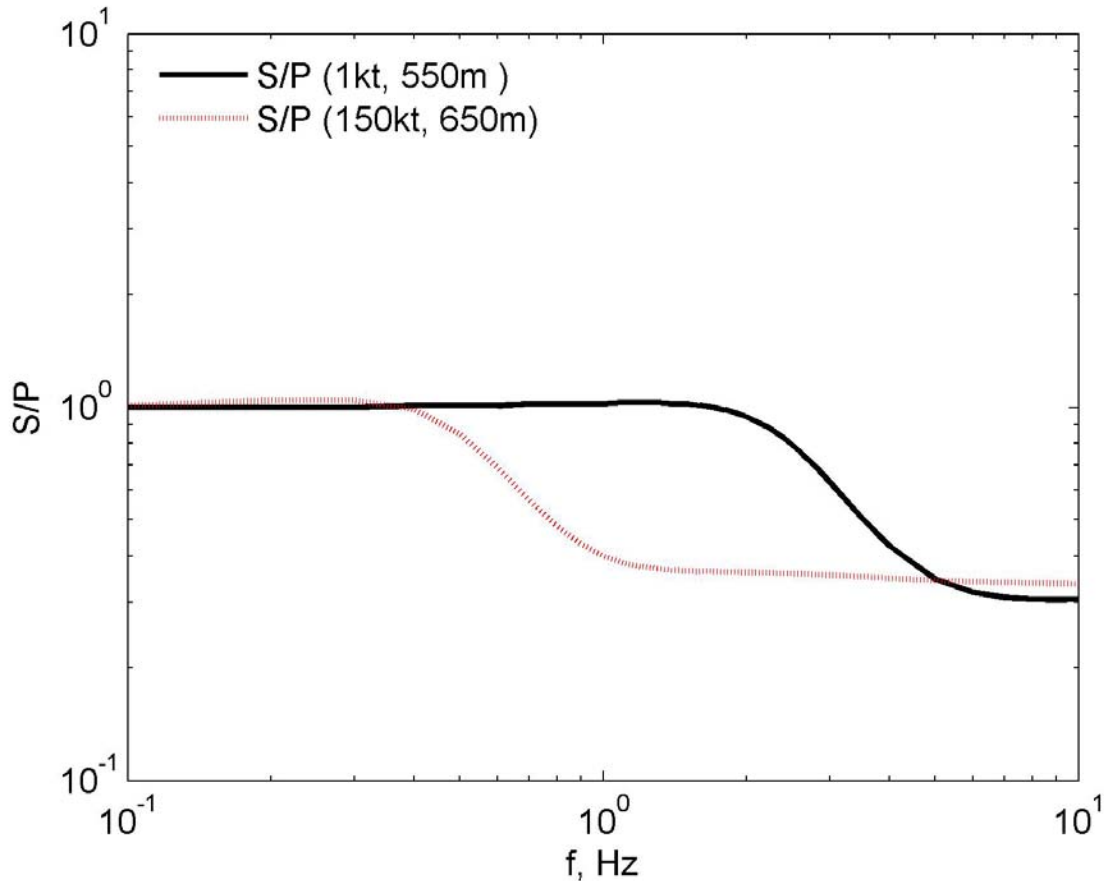


Figure 34. Comparison of theoretical S/P source spectral ratios predicted by the Mueller/Murphy based model for an overburied explosion in saturated tuff with a yield of 1 kt and a depth of burial of 550m and an explosion with a yield of 150 kt and a depth of burial of 650m.

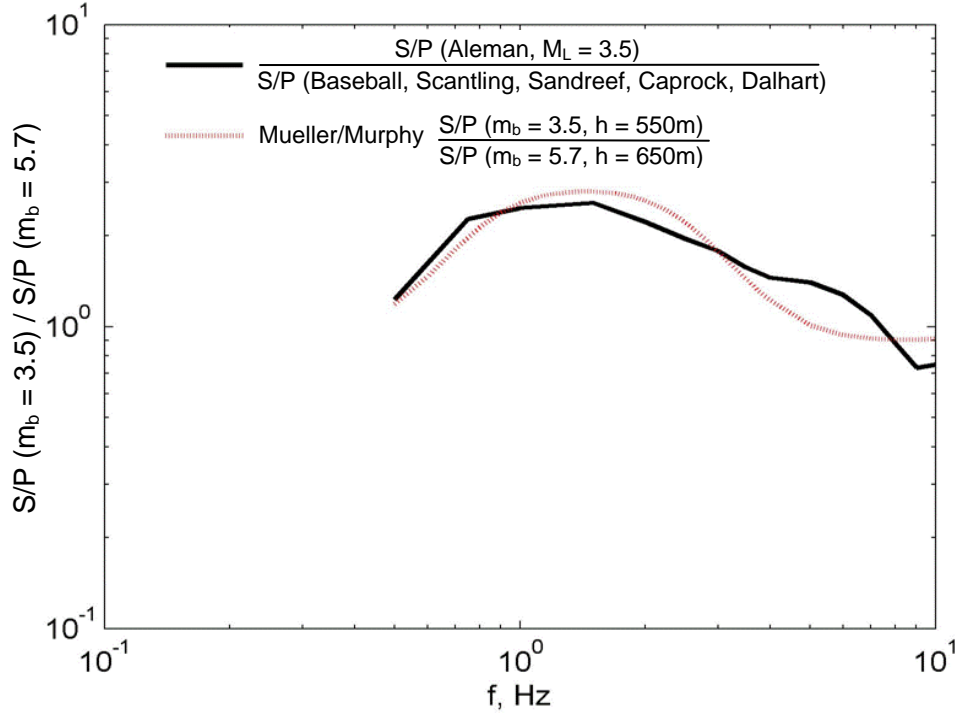


Figure 35. Comparison of the ratio of the observed Aleman S/P ratio to the average S/P ratio for five larger Yucca Flat explosions having a mean m_b value of about 5.7 with the corresponding theoretical ratio predicted by the Mueller/Murphy based model.

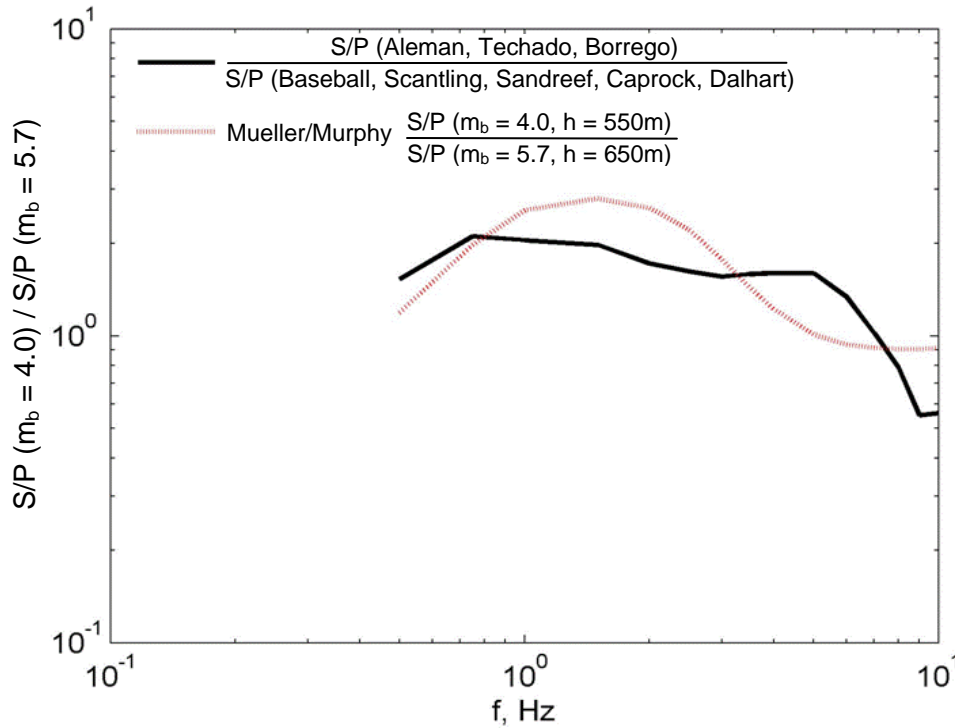


Figure 36. Comparison of the ratio of the average observed S/P spectral ratio for the three smallest Yucca Flat explosions having a mean m_b value of about 4.0 to the average observed S/P spectral ratio for five Yucca Flat explosions having a mean m_b value of about 5.7 with the corresponding theoretical ratio predicted by the Mueller/Murphy based model.

As was noted above, data recorded at these four LLNL network stations also provide an excellent basis for assessing possible azimuthal dependence of the seismic sources of the various observed regional seismic phases. For example, Figure 37 shows a comparison of the ratios of the observed S/P ratios at station MNV to the corresponding network-averaged S/P ratios as a function of frequency for the selected sample of seven Yucca Flat explosions. In the absence of variations in the S/P radiation patterns from one explosion to the next, it would be expected that this ratio would remain essentially constant from event to event, and equal to the difference between the frequency dependent propagation path effects to station MNV relative to the network-averaged propagation effects for the four LLNL stations. In fact, it can be seen from this figure that these ratios are very consistent, which constrains any variations in the S/P radiation patterns from event to event to be quite small. It follows that the average (logarithmic) of these ratios should give a good estimate of the MNV frequency dependent "station correction" relative to the network average. The results of computing such averages for the same sample of seven explosions at each of the four LLNL stations are shown in Figure 38, where it can be seen that they are remarkably consistent. It can be concluded from these results that the total average effect of both propagation path differences and any source azimuthal variations on S/P is only on the order of 20% over the entire analyzed frequency band from 0.5 to 8.0 Hz for these four LLNL stations. That is, the consistency shown in Figure 38 places very strong constraints on any proposed S wave generation mechanism for these explosions, particularly with regard to allowable azimuthal variability of the S wave seismic source.

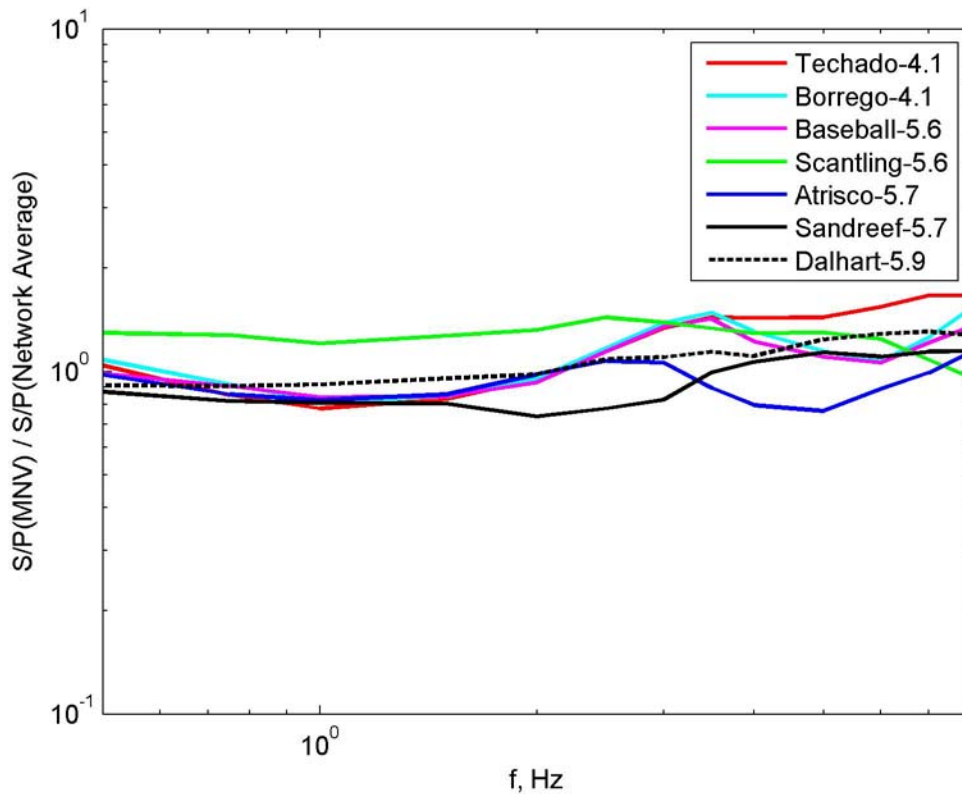


Figure 37. Ratios of station MNV S/P spectral ratios to corresponding network-averaged S/P spectral ratios for selected Yucca Flat explosions.

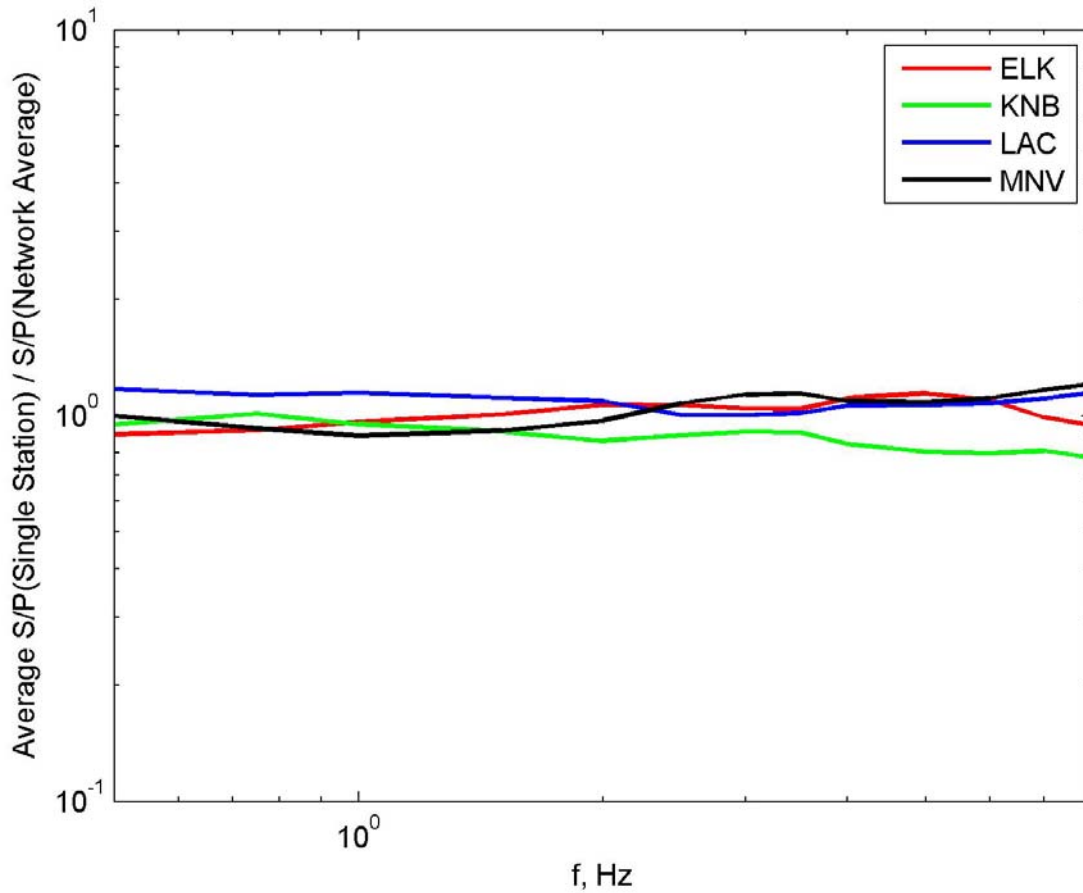


Figure 38. Average ratios of single station S/P spectral ratios to corresponding network-averaged S/P spectral ratios for LLNL stations ELK, KNB, LAC and MNV.

5. CONCLUSIONS

The principal objective of the studies summarized in this report has been to derive improved, quantitative constraints on proposed physical mechanisms for S wave generation by explosion sources. This has been accomplished through a systematic evaluation of the frequency dependent source scaling characteristics of regional phase data observed from underground nuclear explosions at the former Soviet Semipalatinsk test site, the Chinese Lop Nor test site, the Russian Novaya Zemlya test site and the U.S. NTS test site. The source scaling results for all these testing areas have been found to be remarkably consistent, indicating that the observed Sn and Lg spectra scale with yield in a manner which is very comparable to that of the corresponding direct Pn spectra, generally differing significantly only over narrow frequency bands defined by differences in the P and S wave corner frequencies. Moreover, direct comparisons of Sn/Pn and Lg/Pn spectral ratios over the sampled ranges of depth and scaled depth indicate that any differences in the frequency dependent source depth dependencies of Pn, Sn and Lg must also be rather small. More specifically, it has been found that the observed frequency dependent source scaling of S/P spectral ratios at each of these test sites is very consistent

with the simple phenomenological model proposed by Fisk et al(2005) in which the S wave source is obtained from the corresponding Mueller/Murphy P wave source by scaling the corner frequency by the S/P velocity ratio of the source medium. While these results have not yet led to the identification of a specific physical mechanism for S wave generation by explosions, they do provide strong constraints which must be satisfied by any plausible proposed physical mechanism. In particular, any such physical mechanism for S wave generation at these test sites must satisfy the following observational constraints:

- (1) the characteristic source length for S is comparable to that for P, independent of yield, depth of burial or source medium.
- (2) the frequency dependent S/P source excitation ratio is approximately constant for explosions at a fixed test site, independent of yield or scaled depth of burial.
- (3) the frequency dependent S/P source spectral ratio is approximately independent of source to station azimuth over the frequency band extending from about 0.5 to 10 Hz.

It is recommended that all proposed source models for S wave generation by explosions be used to predict frequency dependent S/P ratios as functions of explosion yield and depth of burial, as well as source to station azimuth, to determine whether they are compatible with these quantitative observational constraints.

REFERENCES

- Adushkin, V. V. and V. A. An (1990), "Seismic Observations and Monitoring of Underground Nuclear Explosions at Borovoye Geophysical Observatory," *Izv. Acad. Sci. USSR, Phys. Solid Earth*, 12, 1023-1031.
- Archambeau, C. B. (1972), "The Theory of Stress Wave Radiation From Explosions in Prestressed Media," *Geophys. J. R. Astr. Soc.*, 29, 329-366.
- Bennett, T. J. and J. R. Murphy (1986), "Analysis of Seismic Discrimination Capabilities Using Regional Data From Western U. S. Events," *Bull. Seism. Soc. Am.*, 76, pp. 1006-1021.
- Bycroft, G. N. (1966), "Surface Displacements Due to an Underground Explosion," *Bull. Seism. Soc. Am.*, 56, pp. 877-892.
- Fisk, M. D., D. Jepsen and J. R. Murphy (2002), "Experimental Seismic Event-screening Criteria at the Prototype International Data Center," *Monitoring the Comprehensive Nuclear-Test-Ban Treaty: Discrimination*, PAGEOPH Topical Volume, Birkhauser, pp. 865-888.
- Fisk, M. D., S. R. Taylor and T. Lay (2005), "Modeling and Empirical Research on Energy Partitioning of Regional Seismic Phases Used For Explosion Monitoring," in *Proceedings of the 27th Seismic Research Review*, Rancho Mirage, CA September 20-22.
- Given, J. W. and G. R. Mellman (1986), "Estimating Explosion and Tectonic Release Source Parameters of Underground Nuclear Explosions From Rayleigh- and Love-wave Observations," *Sierra Geophysics Final Report to Air Force Geophysical Laboratory, Part 1*, AFGL-TR-86-0171, SGI-R-86-126, July.
- Gupta, I. N., T. W. McElfresh, and R. A. Wagner (1991), "Near-Source Scattering of Rayleigh to P in Teleseismic Arrivals From Pahute Mesa NTS Shots," in *Explosion Source Phenomenology*, AGU Monograph 65, 151-159.
- Gupta, I. N., T. Zhang, and R. Wagner (1977), "Low-Frequency Lg From NTS and Kazakh Nuclear Explosions – Observations and Interpretations," *Bull. Seism. Soc. Am.*, 87, 1115-1125.
- Jih, R. S., and K. L. McLaughlin (1988), "Investigation of Explosion Generated SV Lg Waves in 2-D Heterogeneous Crustal Models by Finite-Difference Method," Report No. AFGL-TR-88-0025.
- Mueller, R. A. and J. R. Murphy (1971), "Seismic Characteristics of Underground Nuclear Detonations, I: Seismic Spectrum Scaling," *Bull. Seism. Soc. Am.*, 61, pp. 1675-1692.
- Murphy, J. R. (1973), "Rayleigh Waves From a Nuclear Source in a Halfspace," *NVO*-1163-238.
- Murphy, J. R. (1977), "Seismic Source Functions and Magnitude Determinations for Underground Nuclear Detonations," *Bull. Seism. Soc. Am.*, 67, pp. 135-158.
- Murphy, J. R. (1981), "P-Wave Coupling of Underground Explosions in Various Geologic Media," in *Identification of Seismic Sources - Earthquake or Underground Explosion*, Proceedings of the NATO Advanced Study Institute, D. Reidel Publishing Company.

- Murphy, J. R., B. W. Barker and A. O'Donnell (1989), "Network-Averaged Teleseismic P-Wave Spectra For Underground Explosions, I: Definitions and Examples," *Bull. Seism. Soc. Am.*, 79, pp. 1-15.
- Murphy, J. R. (1996), "Types of Seismic Events and Their Source Descriptions," in *Monitoring a Comprehensive Test Ban Treaty*, Proceedings of the NATO Advanced Study Institute, Kluwer Academic Publishers, pp. 225-245.
- Murphy, J. R., I. O. Kitov, B. W. Barker and D. D. Sultanov (2001), "Seismic Source Characteristics of Soviet Peaceful Nuclear Explosions," *Monitoring the Comprehensive Nuclear-Test-Ban Treaty: Source Processes and Explosion Yield Estimation*, PAGEOPH Topical Volume, Birkhauser, pp. 2077-2101.
- Murphy, J. R., and B. W. Barker (2001), "Application of Network-Averaged Teleseismic P Wave Spectra to Seismic Yield Estimation of Underground Nuclear Explosions," *Monitoring the Comprehensive Nuclear-Test-Ban Treaty: Source Processes and Explosion Yield Estimation*, PAGEOPH Topical Volume, Birkhauser, pp. 2123-2171.
- Nuttli, O. W. (1986). "Yield Estimates of Nevada Test Site Explosions Obtained from Seismic L_g Waves," *J. Geophys. Res.*, 91, pp. 2137-2151.
- Office of Technology Assessment (1988), *Seismic Verification of Nuclear Testing Treaties*, OTA-SC-361, Government Printing Office, Washington, D. C.
- Stevens, J. L., T. G. Barker, S. M. Day, K. L. McLaughlin, N. Rimer, and B. Shkoller (1991), "Simulation of Teleseismic Body Waves, Regional Seismograms, and Rayleigh Wave Phase Shifts Using Two-Dimensional Nonlinear Models of Explosion Sources," *AGU Geophysical Monograph 65: Explosion Source Phenomenology*, S. Taylor, H. Patton, P. Richards, editors, ISBN 0-87590-031-3, pp. 239-252.
- Stevens, J. L., G. E. Baker, H. Xu, T. J. Bennett, N. Rimer and S. M. Day (2003), "The Physical Basis of L_g Generation by Explosion Sources," in *Proceedings of the 25th Seismic Research Review - Nuclear Explosion Monitoring: Building the Knowledge Base*, LA-UR-03-6029.
- Taylor, S. N. Sherman, and M. Denny (1988), "Spectral Discrimination Between NTS Explosions and Western United States Earthquakes at Regional Distances," *Bull. Seism. Soc. Am.*, 78, 1563-1579.